OFFICE OF NAVAL RESEARCH

Contract No. N00014-91-J-1409

Technical Report No. 115

Dynamical Solvent Effects on Activated Electron-Transfer Reactions: Principles, Pitfalls, and Progress

by

Michael J. Weaver

Prepared for Publication

in

Chemical Reviews

Purdue University

Department of Chemistry

West Lafayette, Indiana 47907

February 1992

SECURITY CLASSIFICATION OF THIS PAGE

REPORT DOCUMENTATION PAGE

Form Approved OMB No. 0704-0188

1a. REPORT SECURITY CLASSIFICATION Unclassified	1b. RESTRICTIVE MARKINGS
2a. SECURITY CLASSIFICATION AUTHORITY	3. DISTRIBUTION/AVAILABILITY OF REPORT Approved for public release and sale; its distribution is unlimited.
2b. DECLASSIFICATION/DOWNGRADING SCHEDULE	
4. PERFORMING ORGANIZATION REPORT NUMBER(S) Technical Report No. 115	5. MONITORING ORGANIZATION REPORT NUMBER(S)
6a. NAME OF PERFORMING ORGANIZATION Purdue University Department of Chemistry 6b. OFFICE SYMBOL (If applicable)	7a. NAME OF MONITORING ORGANIZATION Division of Sponsored Programs Purdue Research Foundation
6c. ADDRESS (City, State, and ZIP Code) Purdue University Department of Chemistry West Lafayette, IN 47907	7b. ADDRESS (City, State, and ZIP Code) Purdue University West Lafayette, IN 47907
8a. NAME OF FUNDING/SPONSORING ORGANIZATION Office of Naval Research 8b. OFFICE SYMBOL (If applicable)	9. PROCUREMENT INSTRUMENT IDENTIFICATION NUMBER Contract No. N00014-91-J-1409
8c. ADDRESS (City, State, and ZIP Code) 800 N. Quincy Street Arlington, VA 22217	10. SOURCE OF FUNDING NUMBERS PROGRAM ELEMENT NO. / PROJECT NO. / TASK NO / WORK UNIT ACCESSION NO.

11. TITLE (Include Security Classification)
Dynamical Solvent Effects on Activated Electron-Transfer Reactions: Principles, Pitfalls, and Progress

12. PERSONAL AUTHOR(S)
Michael J. Weaver

13a. TYPE OF REPORT	13b. TIME COVERED	14. DATE OF REPORT (Year, Month, Day)	15. PAGE COUNT
Technical	FROM _____ TO _____	February 28, 1992	

16. SUPPLEMENTARY NOTATION

17. COSATI CODES			18. SUBJECT TERMS (Continue on reverse if necessary and identify by block number)
FIELD	GROUP	SUB-GROUP	separation of dynamical and energetic factors, solvent-friction effects, rapid solvent relaxation components, reactant intramolecular dynamics, activation-parameter analyses.

19. ABSTRACT (Continue on reverse if necessary and identify by block number)

Recent experimental and conceptual progress in our understanding of dynamical solvent effects in activated electron-transfer processes are critically reviewed.

20. DISTRIBUTION/AVAILABILITY OF ABSTRACT ☐ UNCLASSIFIED/UNLIMITED ☐ SAME AS RPT. ☐ DTIC USERS	21. ABSTRACT SECURITY CLASSIFICATION
22a. NAME OF RESPONSIBLE INDIVIDUAL	22b. TELEPHONE (Include Area Code) / 22c. OFFICE SYMBOL

DD Form 1473, JUN 86 Previous editions are obsolete. SECURITY CLASSIFICATION OF THIS PAGE

CONTENTS

Michael J. Weaver was born in London, England, in 1947. Following doctoral research at Imperial College with Dr. Douglas Inman, he was a research fellow at Caltech under Prof. Fred Anson from 1972 to 1975. After a period on the faculty at Michigan State University, he moved to Purdue University in 1982 where he has been Professor of Chemistry since 1985. His research interests span electrochemistry, electron-transfer chemistry, surface vibrational spectroscopies, and electrochemical surface science. He is continually amazed by (and grateful for) the diversity of research disciplines, and inspiring scientific colleagues, that a physical electrochemist can stumble upon.

I. Introduction

Understanding the various influences exerted by the solvating environment upon the kinetics of electron-transfer (ET) processes, either in homogeneous solution or at metal-solution and related interfaces, has long captured the attention of experimentalists and theoreticians alike. Traditionally, these roles have been perceived primarily in terms of *energetic* factors, whereby the solvent is considered to affect the reaction rates via its influence on the net activation barrier to electron transfer, ΔG^*. Indeed, such considerations form a mainstay of the well-known Marcus and related theoretical treatments.[1] In these approaches, solvent effects upon ΔG^* are separated into so-called intrinsic and extrinsic (or thermodynamic) factors. The latter encompasses the various solvent influences upon ΔG^* attributed to the reaction free energy, ΔG°, whereas the former describes the barrier component present even in the absence of this driving force.

The physical origin of the intrinsic solvent (or "outer-shell") barrier, ΔG^*_{os} , is in the need for reorganization of surrounding solvent dipoles to occur to some extent prior to the (essentially instantaneous) electron-transfer act itself. Description of ΔG^*_{os} in terms of the conventional dielectric-continuum model leads to well-known expressions, based on a nonequilibrium "Born-charging" treatments, that contain the so-called Pekar factor $(\epsilon_{op}^{-1} - \epsilon_o^{-1})$, where ϵ_{op} and ϵ_o are the optical (infinite frequency) and static (zero frequency) solvent dielectric constants, respectively.[1] For polar solvents, $\epsilon_{op} \ll \epsilon_o$, since the latter quantity contains dominant additional contributions from orientational and vibrational solvent polarization; these components are absent in ϵ_{op} because only electronic polarization influences the solvent dielectric properties at optical frequencies. This circumstance leads to a numerical dominance of the Pekar factor, and hence the predicted ΔG^*_{os} values, by ϵ_{op} rather than ϵ_s. Perhaps

paradoxically, then, the intrinsic reorganization energetics are anticipated to be influenced only mildly by the "slow" nuclear solvent modes.

In addition to such energetic factors, however, one might anticipate that such "slow" solvent repolarization as well as other nuclear reorganization modes that constitute the ET barrier could affect the reaction rate via their influence on the nuclear barrier-crossing frequency ν_n. This latter issue has been discussed most often recently for activationless (sometimes termed "solvent controlled") ET reactions, where $\Delta G^* \approx 0$, so that the solvent relaxation dynamics alone determine the reaction rate. We focus here instead on *activated* ET processes, i.e., those featuring significant ($\gtrsim$ 2 kcal mol^{-1}) free-energy barriers. While solvent dynamics can also exert important influences on the latter reaction type, the anticipated nature of the effects are often quite different to the activationless case.

In the usual transition-state theory (TST) format, one can express the (unimolecular) rate constant, k_{et}, for activated ET as[2]

$$k_{et} = \kappa_{el}\nu_n \exp(-\Delta G^*/k_BT) \quad (1)$$

where k_B is the Boltzmann constant, and κ_{el} is the electronic transmission coefficient. For sufficient donor-acceptor electronic coupling so that $\kappa_{el} \to 1$, "adiabatic" pathways prevail so that the ET barrier-crossing frequency will be controlled entirely by ν_n. The usual TST expression for ν_n is[2]

$$\nu_n = (\sum \nu_j^2 \Delta G_j^*/\Delta G^*)^{1/2} \quad (2)$$

where ν_j is the harmonic frequency of the jth nuclear mode which contributes to the overall barrier ΔG^* to an extent equal to ΔG_j^*. This expression indicates that the molecular rotational and other individual nuclear motions associated with solvent reorganization can influence ν_n and hence the reaction rate,

although the form of Eq(2) suggests that higher-frequency modes (especially vibrations) should often dominate ν_n. The latter is anticipated to be the case for reactions where reactant intramolecular (i.e., inner-shell) distortions form a significant or substantial component of the activation barrier in addition to solvent (i.e., outer-shell) reorganization.

Over the last decade, however, it has become apparent that dynamical solvent properties can influence the rates of electron-transfer, as well as other chemical, processes in a distinctly more intricate and molecularly sensitive fashion. This recognition forms part of the broadbased theoretical development and associated experimental examination of so-called solvent "friction" effects in chemical kinetics.[3] The physical origin of these effects resides in the *collective* solvent motion which is encountered as a requirement for barrier crossing in many chemical processes, such as isomerizations and atom or group, as well as charge, transfers. The essential (albeit perhaps vague) general notion behind solvent friction is that the required collective solvent motion impedes progress along the reaction coordinate below the frequency characterizing the reactant subsystem. Rather than the solvent "bath" acting as an obedient reversible energy source or sink, as in the TST picture, irreversible reactant-solvent energy dissipation is perceived to occur, diminishing the net rate for passage up and over the barrier below the TST-anticipated value.[3]

The physical nature of solvent friction in activated as well as activationless ET processes is somewhat different in that the solvent itself can form an important contributor to the reaction coordinate as well as providing the "energy bath", and indeed is the sole component of the activation barrier for reactions where reactant intramolecular distortions are absent. In this latter case, the "reactant mode" frequency for activated ET (and hence the free-energy well frequency ω_o) are related closely to the rotational time of individual solvent

dipoles, τ_{rot}. A simple TST formulation for this purpose is[4]

$$\nu_n = \frac{\omega_o}{2\pi} = (2\pi\tau^s_{rot})^{-1}\left(\frac{2\epsilon_o + \epsilon_\infty}{3\epsilon_\infty g_k}\right)^{1/2} \quad (3a)$$

$$= (2\pi\tau_{rot})^{-1} \quad (3b)$$

where ϵ_∞ is the so-called "infinite frequency" dielectric constant and g_k is the Kirkwood "g" factor, both characterizing the solvent dielectric medium, and τ^s_{rot} is the "free" (gas-phase) solvent inertial rotation time, as extracted from microwave spectra. The combined square-root term in Eq(3a) prescribes the alteration to the rotational time of individual solvent molecules induced by the surrounding dielectric medium, yielding the *solvent-phase* inertial rotation time τ_{rot} [Eq(3b)].

The presence of surrounding solvent molecules, however, can also diminish the effective frequency of the *collective* solvent motion required to move significantly along the ET reaction coordinate (and hence over the barrier top) well below this TST value, again by means of irreversible energy dissipation of the "reactant" solvent dipole to the surrounding solvent "bath." So-called "overdamped" solvent dynamics are obtained. This phenomenon, in general terms, encompasses the notion of "dielectric friction" by which the rates of ET processes can be impeded in polar media. While the familiar form of the TST-like expression Eq(1) is still applicable under these circumstances [at least for $\Delta G^* \gtrsim (2\text{-}3)k_BT$], the rate will be depressed as a result of barrier-crossing frequencies, ν_n, which are smaller than the TST value, $\omega_o/2\pi$. For reaction barriers featuring significant contributions from intramolecular reactant (inner-shell) reorganization, dielectric friction can also act in a fashion more akin to other chemical processes by limiting the rate at which solvent configurations

corresponding to reactant subsystem energies close to the barrier top are achieved, thereby impeding consequent barrier crossing via inner-shell motion (vide infra).

While the general notion of solvent-friction effects in chemical kinetics has its origins in a paper by Kramers published over a half-century ago,[5] theoretical development has occurred only much more recently. The initial application of dielectric-friction concepts to activated electron-transfer processes, by Zusman, appeared in 1980.[6] Since then, there has been a veritable deluge of analytic theoretical papers on this topic (see refs. 7-15, along with recent reviews,[16] for a short representative selection). Related molecular-dynamical (MD) computational studies have also begun to appear.[17]

In the wake of this high degree of theoretical activity, it is of particular interest to explore experimentally the manner and extent of dynamical solvent effects on electron transfer in comparison with the theoretical predictions. Spawned by the recent development of ultrafast laser techniques, a number of studies of photoinduced intramolecular charge-transfer reactions have been reported in which the rates appear to be dominated by the solvent dynamics, the reactions being close to activationless in nature.[18] Related measurements of time-dependent fluorescence Stokes shifts (TDFS) for chromophores forming suitable dipolar excited states have enabled the real-time dynamics of dipolar solvation to be examined directly.[18a,19] These measurements have provided a detailed assessment of the strengths and limitations of both dielectric continuum and molecularly based models of overdamped solvent-relaxation dynamics. While providing invaluable experimental information on polar solvation dynamics of relevance to both activationless and activated ET processes, it is clearly also of importance to explore directly the possible roles of solvent dynamics on the latter class of reaction. The significance of this quest is highlighted by the

knowledge that the vast majority of electron-transfer systems are activated, i.e., feature free-energy barriers of several k_BT or more.

A central complication in exploring experimentally solvent dynamical effects for such activated processes, however, is that the measured rates are commonly influenced substantially (or even predominantly) by the activation energetics as well as dynamics, as reflected in the ΔG^* and ν_n terms, respectively, in Eq(1). Consequently, the extraction even of semiquantitative estimates of the nuclear frequency factor from rate measurements requires reliable information on the activation energetics. At first sight, the evaluation of so-called activation parameters from temperature-dependent rate parameters might be expected to provide a straightforward separation of such preexponential and exponential kinetic factors. At least for bimolecular reactions, however, this approach often turns out to be far from unambiguous (see below).

In practice, most attempts to extract dynamical information for such activated processes utilize instead solvent-dependent rate measurements for electron-exchange processes (i.e., reactions in which $\Delta G^\circ = 0$).[20] The usefulness of this strategy derives from the expectation that in selected cases the anticipated solvent-dependent variations in ν_n arising from differing solvent dynamics are greater than, or functionally different from, those in the activation energetics factor $\exp(-\Delta G^*/k_BT)$. At least for judiciously chosen systems, this strategy can lead to the extraction of relatively reliable experimental information on solvent dynamical effects for homogeneous self exchange and, to a lesser extent, for electrochemical exchange reactions.[20]

One specific aim of this article is to provide a critical assessment of the virtues and limitations of such experimental approaches, along with an overview of the dynamical information thus obtained in comparison with contemporary theoretical expectations. Of additional interest is the appraisal of such

solvent dynamics for activated electron-transfer processes in relationship to the detailed knowledge of dielectric relaxation that has become available from ultrafast laser, as well as from solvent dielectric loss, measurements. Rather than attempt a comprehensive review of experimental and theoretical work in this multifaceted (and often esoteric) area, the overall emphasis here is on providing a (hopefully) straightforward survey of the underlying physical concepts and experimental insight on solvent dynamical effects as they impact on our fundamental understanding of activated ET kinetics on a more general basis. A practical issue addressed herein is the degree to which solvent-dependent kinetic analyses can be utilized to gain *reliable* information of this type; unfortunately, such procedures have sometimes been applied uncritically in the recent literature.

A briefer overview of some of these issues is to be found in ref. 20. Attention is also drawn to the article by Hynes in this issue of Chemical Reviews which deals with some recent theoretical and computational aspects of dynamical solvent effects in electron transfer.[21]

II. Conceptual Kinetic Framework

We consider here homogeneous-phase and electrochemical ET reactions, proceeding via outer-sphere mechanisms, having the general forms

$$Ox_1 + Red_2 \rightarrow Red_1 + Ox_2 \qquad (4)$$

$$Ox_1 + \text{electrode (E)} \rightarrow Red_1 \qquad (5)$$

where Ox and Red refer to oxidized and reduced forms of a given redox couple. Primary attention will be focussed on homogeneous self-exchange processes (where $Ox_1 = Ox_2$, $Red_1 = Red_2$), and related electrochemical exchange reactions (for which the electrode potential E equals the standard potential E°). In both cases ΔG°

= 0, thereby removing driving-force contributions to the activation barrier. Under these conditions, most of the conceptual discussion below applies interchangeably to both homogeneous-phase and electrochemical processes, although the distinct features of both reaction types will be emphasized whenever appropriate.

The observed rate constant, k_{ob}, for either homogeneous-phase or heterogeneous (electrochemical) ET processes can be related to the unimolecular rate constant in Eq(1) most simply by[2,22]

$$k_{ob} = K_p k_{et} \tag{6}$$

where K_p is a preequilibrium constant which describes the statistical probability of finding the reactant (or reactant-electrode) pair in an internuclear configuration appropriate for reaction.[23] (This term can also contain appropriate electrostatic work-term corrections.) In general, a distribution of internuclear geometries, each having different formation probabilities (K_p) and "local" unimolecular rate constants (k_{et}), will contribute to k_{ob}, with the form of the required integral depending on the reactant geometries. Thus for a pair of "ideal spherical" reactants:[24]

$$k_{ob} = \left(\frac{4\pi N}{10^3}\right) \int_{r_o}^{\infty} r^2 \, k_{et}(r) \, g_{DA}(r) \, dr \tag{7}$$

where r is the reactant internuclear distance with r_o referring to contact, N is the Avogadro number, and g_{DA} is an appropriate radial distribution function. [A corresponding relation can be written for electrochemical processes, involving a single reactant (and a planar surface) by replacing the spherical with linear r coordinates.[25]] The g_{NA} term is usually set equal to unity, which is tantamount to assuming that the reactant electronic interactions (orbital

overlap, etc.) exhibit simple spherical isotropy, and the solvent can be perceived as a structureless continuum. (Examples where this is clearly not the case are considered below.) Even in the presence of molecular anisotropy, however, the observed bimolecular rate constant is often expected to reflect a sufficiently narrow range of precursor geometries so that the kinetics may be described approximately by singular values of k_{et}, ν_n, κ_{el}, ΔG^*, and K_p. Under these circumstances, Eq(6) can provide a useful means of describing the observed rate constant. In this case, one can combine Eqs(1) and (6) to yield the following overall expression for the electron-exchange rate constant, k_{ex}:

$$k_{ex} = K_p \kappa_{el} \nu_n \exp\left(\frac{-\Delta G_i^*}{k_B T}\right) \tag{8}$$

where ΔG_i^* is the "intrinsic" barrier (i.e., when $\Delta G^\circ = 0$).

This simplified formula provides a convenient starting point for outlining the basic features of solvent-dependent dynamical effects upon k_{ex} as anticipated from theoretical models, along with appropriate experimental analyses for exploring them. As already noted, the influence of solvent dynamics upon k_{ob} is contained within the nuclear frequency factor ν_n. The simplest case is where virtually the entire barrier arises from solvent reorganization, i.e., where the inner-shell contributions are small or negligible. Following the format of Eq(3b), we can define an "effective" solvent relaxation time for barrier crossing, τ_{eff}, so that $\nu_n = (2\pi\tau_{eff})^{-1}$. In the presence of solvent friction (overdamped solvent relaxation), $\tau_{eff} > \tau_{rot}$, so that the observed reaction rate will fall below that expected for the TST limit.

Of central interest are the possible connections between τ_{eff} and the various solvent relaxation times observed in TDFS measurements or extracted from solvent dielectric loss spectra. For exchange reactions featuring a cusp (i.e.,

sharp) barrier top as expected for weak donor-acceptor electronic coupling, a dielectric-continuum treatment predicts that[6,7a,26]

$$\nu_n = \tau_L^{-1} \, (\Delta G^*_{os}/4\pi k_B T)^{1/2} \tag{9}$$

where ΔG^*_{os} is the intrinsic "outer-shell" barrier associated with solvent reorganization, and where τ_L is the well-known longitudinal solvent relaxation time. The latter is usually extracted from the Debye relaxation time, τ_D, obtained in dielectric-loss spectra by[27,28]

$$\tau_L = (\epsilon_\infty/\epsilon_o)\tau_D \tag{10}$$

From the form of Eq(9), for reactions featuring moderate (say 4-8 kcal mol^{-1}) barriers as anticipated in polar solvents at ambient temperatures, $\nu_n \sim \tau_L^{-1}$, so that roughly $\tau_{eff} \sim \tau_L/2\pi$. For most common solvents at ambient temperatures, $\tau_L^{-1} < \tau_{rot}^{-1}$ and hence $\tau_L^{-1} < \omega_o$ [Eq(3b)]. Some representative comparisons between τ_L^{-1} and ω_o as estimated from Eq(3) are contained in Table I.

Consequently, then, in the presence of such overdamped solvent relaxation one can anticipate commonly that $\tau_{eff}^{-1} \ll \tau_{rot}^{-1}$, so that substantial rate retardations below the TST limit are usually expected on this basis. Additional inspection of Table I shows that, significantly, the τ_L^{-1} values are markedly more sensitive to the solvent nature than ω_o; for example, the former quantity is 20-fold smaller for benzonitrile than acetonitrile. This solvent structural sensitivity of τ_L, which is observed more generally,[29] suggests that the barrier-crossing frequency may be changed substantially by altering the solvent medium. A qualitatively similar conclusion can be reached on the basis of the solvation relaxation times, τ_s, extracted from TDFS measurements; comparisons between τ_L and τ_s will be considered further below.

Unlike the TST case, the barrier-crossing frequency in the presence of

solvent friction is generally expected to be dependent not only on the barrier height ΔG^{*}_{os} [Eq(9)] but also on the shape of the barrier top. The latter is influenced by the degree of donor-acceptor orbital overlap as gauged by the electronic coupling matrix element, H_{12}; in the cusp-barrier limit, $H_{12} = 0$, with the barrier top becoming more "rounded" as H_{12} increases.[2] The relation between H_{12} and the ET barrier for a symmetrical exchange reaction is illustrated schematically in Fig. 1. In the presence of solvent friction, ν_n is expected to diminish monotonically as the barrier-top roundedness increases.[7a,8c,30] For barrier shapes typical for activated outer-sphere ET, ν_n is predicted to be somewhat (ca 2-5 fold) smaller than the cusp-limit value, ca τ_L^{-1}.[30] A simple physical rationalization of this barrier-shape effect derives from the notion that solvent friction acts to diminish the net frequency factor ν_n in part by the barrier *recrossings*, or incomplete crossings, induced by such dissipative relaxation.[3a,b] As the barrier top broadens, therefore, the frequency of successful diffusive passages through this region should become progressively smaller. A simple, yet effective, treatment of Hynes[8c] sets the inverse net barrier-crossing frequency equal to the reciprocal sum of the rates for ascending the reactant well, k_w, and traversing the barrier top, k_b. Although both k_w and k_b can be diminished in the presence of solvent friction; the latter diminishes as H_{12} increases, and is thereby more likely to become rate controlling under these conditions.

On the basis of the foregoing, then, there is reason to believe that rate measurements for suitable electron-exchange reactions in judiciously chosen series of solvents should yield substantial insight into the nature and extent of dynamical solvent effects, providing that sufficient information is available on the solvent-dependent ET barrier heights. This notion is indeed borne out under some circumstances. Prior to discussing further the virtues and pitfalls

of such solvent-dependent analyses, it is necessary to consider several additional features which together may conspire to make the influence of solvent dynamics on the reaction rate rather more involved than suggested by relations such as Eq(9). The most important of these factors will now be briefly described in turn.

(i) *High-frequency solvent dispersions.* Even within the dielectric continuum limit, many solvents exhibit additional dispersions in the dielectric loss spectra at higher frequencies than the "major" Debye relaxation, τ_D.[27] In such cases, the relaxation dynamics are nonexponential and no longer described entirely by τ_L, as extracted from Eq(10). The observation of such "non-Debye" behavior in dielectric loss spectra has undoubtedly been limited by the frequency ranges over which such measurements have commonly been undertaken,[27] so that its occurrence may be much more common than is apparent from published data. Nevertheless, the clear observation of such high-frequency dissipative relaxations has been made in a number of solvents, most notably in primary alcohols.[31]

(ii) *Noncontinuum (solvent molecularity) effects.* Even in the absence of multiple dissipative components for the pure solvent, there are good reasons to anticipate that τ_L can provide only an incomplete description of solvent relaxation in the vicinity of the reacting solute. Part of this evidence is derived from a number of theoretical examinations of "solvent molecularity" effects emanating from the inevitable limitations of dielectric-continuum treatments for describing local solvation. A simple approach to considering such molecular solvation effects is to utilize the mean spherical approximation (MSA) which treats the solvent as hard spheres with imbedded dipoles. A number of recent theoretical examinations along these lines stemmed from the demonstration by Wolynes that the MSA model could be utilized in a nonequilibrium fashion to

treat the dynamics and energetics of solvent-controlled reactions.[7b] This approach applied to Debye solvents yields a spatial distribution of solvent relaxation times, increasing from τ_L far from the reacting solute to values close to τ_D at short distances.[7b,10b] (This spatial dependence was predicted originally by Onsager in 1977.[32])

There has been considerable interest in comparing such dynamical MSA predictions with experimental TDFS relaxation times, τ_s (see refs. 18a, 19a,b for recent reviews). While initial comparisons suggested that $\tau_s > \tau_L$ in accordance with MSA predictions,[33] it now appears that the observed TDFS behavior is closer to the dielectric-continuum predictions than expected from the MSA model.[18a,19a] One suggested reason for this surprising success of the continuum theory is it arises from a fortuitous compensation between the influence of solvent molecularity and dipole translational motion.[19a] As shown by van der Zwan and Hynes[8b] and latterly by Bagchi et al,[15] solvent dipolar translational as well as rotational motion can contribute importantly to the relaxation dynamics under some conditions. However, the relative lack of success of the MSA model may well be due also to its inability to account for specific solvent-solvent interactions.

Of particular interest is the recent observation by Barbara et al of "fast" (subpicosecond) relaxation components in a number of solvents by means of TDFS measurements using coumarin solute probes.[18a,34] Besides the translational motion just noted, there are several theoretical reasons to anticipate the presence of τ_s components markedly shorter than τ_L even in Debye media, arising from short-range solvation and accompanying field inhomogeneity.[35,36] The likely relevance of rapid relaxation components, arising from either non-Debye or short-range solvation, to ET barrier-crossing dynamics is considered below.

(iii) *Reactant vibrational effects.* As already noted, many activated ET processes feature significant or substantial barrier components associated with reactant vibrational or other intramolecular distortions, arising from the differences in reactant bond lengths and angles between the oxidized and reduced states. Given the anticipated common importance of solvent dynamics, a significant issue is the degree to which such effects might be muted in the presence of relatively high-frequency vibrational relaxation. It is important to recognize that Eq(2) above, prescribing the contributions of individual activation modes to ν_n, is inherently a TST expression, thereby requiring that each dynamical component is underdamped.

A distinctly different situation is encountered, however, in the presence of *overdamped* solvent motion. A theoretical treatment describing this latter case has been developed recently by Marcus and coworkers.[9] Some numerical consequences of their approach are considered further below. It is pertinent to note here that the influence of overdamped solvent relaxation upon ν_n is anticipated to be attenuated in the presence of high-frequency reactant modes, in a qualitatively similar fashion to the TST limiting case. Thus the presence of such a rapid underdamped reaction coordinate can provide facile additional channels for barrier passage once the reactant subsystem has reached the vicinity of the barrier top primarily by means of overdamped solvent motion. A key difference, however, is that the overdamped dynamics can exert a significant influence upon ν_n even in the face of a much faster underdamped vibrational coordinate, especially as the former component becomes much slower than the latter. This expectation is quite different to the TST case (vide infra).

(iv) *Reaction nonadiabaticity.* We have so far only considered ET barrier-crossing dynamics in the so-called adiabatic limit, corresponding to $\kappa_{el} \rightarrow 1$ in Eqs(1) and (8), where the donor-acceptor electronic coupling is sufficient so to

oblige the system to remain on a single reaction hypersurface throughout the passage from reactants to products. For the relatively weak electronic coupling (i.e., small H_{12} values) often characterizing outer-sphere ET processes, however, significantly nonadiabatic processes are expected whereby the system is liable to traverse the transition-state region while remaining on the reactant surface. Indeed, in this regard the circumstances leading to Eq(9), involving a cusp-like barrier along with reaction adiabaticity, are somewhat hypothetical.

Besides diminishing the ET reaction rate, the preponderance of such nonreactive "nonadiabatic" transitions can alter drastically the nature of the barrier-crossing dynamics. This is because, unlike the adiabatic limit where the net barrier-crossing frequency $\kappa_{el}\nu_n$ is determined by the dynamics of the various nuclear modes, reactive barrier crossing in the nonadiabatic limit is characterized by an essential *independence* of the rate to the nuclear dynamics, $\kappa_{el}\nu_n$ being controlled instead by the value of H_{12}. Physically, this nonadiabatic barrier passage can be understood most simply in terms of a compensation between the rapidity of motion along the reaction surface and the time, Δt_i, spent within the intersection region of the reactant/product parabolas; the influence of faster nuclear dynamics will be nullified by a correspondingly smaller Δt_i, so that ν_n remains unaffected.

It is desirable to provide an algebraic means of interpolating appropriately between the adiabatic and nonadiabatic limits. In particular, accelerations in the nuclear dynamics as engendered by suitable alterations in the solvent medium (such as increasing τ_L^{-1}) are commonly expected to decrease the degree of reaction adiabaticity, and hence diminish the extent to which ν_n is affected by solvent dynamics. Consequently, then, the solvent-dependent rate behavior that is commonly utilized to explore solvent dynamics can be affected greatly by nonadiabatic effects.[25,29,37] A detailed discussion of appropriate interpolation

formulas is provided in ref. 25; in particular, a treatment was developed which accounts for the coupled influences of nonadiabaticity and barrier-top shape effects upon $\kappa_{el}\nu_n$.

For the present illustrative purposes, a useful expression is the simplified Landau-Zener formula:[2b,25]

$$\kappa_{el} = 2[1 - \exp(-\nu_{el}/2\nu_n)]/[2 - \exp(-\nu_{el}/2\nu_n)] \quad (11)$$

where the "electronic frequency factor" ν_{el} is given by

$$\nu_{el} = (H_{12})^2(\pi^3/\Delta G^* h^2 k_B T)^{1/2} \quad (11a)$$

where h is Plank's constant. For large H_{12} (i.e., strong electronic coupling), $\nu_{el} >> \nu_n$ so that $\kappa_{el} \rightarrow 1$ in Eq(11), and the nuclear dynamics term ν_n in [Eq(1) and (8)] controls entirely the barrier-crossing frequency. On the other hand, for weaker coupling so that $\nu_{el} << \nu_n$, Eq(11) reduces to $\kappa_{el} \approx \nu_{el}/\nu_n$. For such latter "nonadiabatic" circumstances (corresponding to $\kappa_{el} << 1$), the combined preexponential factor $\kappa_{el}\nu_n$ in Eqs(1) and (8) will be *independent* of the nuclear dynamical term ν_n, equaling ν_{el} instead; i.e., proportional to $(H_{12})^2$ ("Golden Rule" limit).

III. Solvent-Dependent Kinetic Analyses: Separation of Dynamical and Energetic Factors

Having outlined some key physical factors that are anticipated to influence the nature of solvent dynamical effects in activated ET processes, we now consider in critical illustrative fashion some solvent-dependent kinetic analyses commonly utilized to extract dynamical information from experimental rate data. Experimental data for self-exchange reactions involving metallocenium-metallocene redox couples will largely be marshalled for this purpose, in view of the uniquely detailed kinetic, energetic, and electronic structural information

available for these solvent dynamical reactant probes.[20] The central issue, and difficulty, involves the separation of the dynamical and energetic components, ν_n and ΔG^*, respectively, in Eq(8), together responsible for the observed solvent-induced variations in k_{ob}. (This presupposes that electrostatic work terms and other K_p components are negligible or otherwise solvent-independent.) A selection of publications from various laboratories where solvent-dependent rate data have been evaluated and analyzed for this purpose, for homogeneous self-exchange and electrochemical exchange processes, are given in refs. 38 and 39, respectively.

The simplest approach used involves the assumption that the observed rate-solvent dependencies are due chiefly to the dynamical component, thereby neglecting the solvent dependence of ΔG^*. There are good reasons, however, to expect that the solvent-dependent dynamical and energetic components are often of roughly comparable magnitude. The latter, intrinsic outer-shell barrier, contribution is usually estimated by means of the following pair of well-known relations, for homogeneous and electrochemical reactions, respectively, derived from dielectric-continuum theory:[1]

$$\Delta G^*_{os,h} = \left(\frac{e^2}{4}\right)\left(a^{-1} - R_h^{-1}\right)\left(\epsilon_{op}^{-1} - \epsilon_o^{-1}\right) \tag{12}$$

$$\Delta G^*_{os,e} = \left(\frac{e^2}{8}\right)\left(a^{-1} - R_e^{-1}\right)\left(\epsilon_{op}^{-1} - \epsilon_o^{-1}\right) \tag{13}$$

Here e is the electronic charge, a is the (spherical) reactant radius, R_h is the internuclear distance in the homogeneous-phase precursor state, and R_e is the corresponding distance between the reactant and its image in the metal electrode.

A key issue is the extent to which Eqs(12) and (13) can provide reliable indicators of at least the *variations* in ΔG^*_{os} with the solvent. There are

several limitations to the application of these relations, not the least of which are the inevitable uncertainties in the appropriate values of the "geometric factors" $(a^{-1} - R_h^{-1})$ and $(a^{-1} - R_e^{-1})$, especially for non-spherical reactants. Moreover, there is theoretical evidence, supported by some experimental kinetic data, to suggest that the "imaging" term in Eq(13) can even be qualitatively inappropriate.[40] The situation, however, for homogeneous-phase processes is somewhat less cloudy, due primarily to the additional availability of *experimental* estimates of ΔG^*_{os}, derived from optical ET energies, ΔE_{op}, observed for intramolecular redox systems.[41] For symmetrical valence-trapped binuclear systems,[41] $\Delta G^*_i = \Delta E_{op}/4$; this simple relation therefore enables the intrinsic outer-shell barrier ΔG^*_{os} in a given solvent to be obtained reliably if the inner-shell component is small or negligible. Provided that the binuclear system represents a close structural analog of the bimolecular self-exchange reaction under study, then, such optical ET data can both circumvent the need to employ theoretical relations such as Eq(12) and also furnish experimental tests of their applicability.

So far, little application of this tactic has been availed in solvent-dependent rate studies. An interesting example along these lines, which has undergone recent detailed examination in our laboratory, involves homogeneous self exchange for metallocenium-metallocene redox couples, of the general form $Cp_2Co^{+/o}$ or $Cp_2Fe^{+/o}$, where Cp is a cyclopentadienyl ring (or derivative thereof).[20] By appropriate derivatization of the Cp ring along with metal substitution, a series of self-exchange reactions can be examined that feature systematic differences in the donor-acceptor electronic coupling.[29,42] Moreover, the redox couples feature small inner-shell barriers, and can be examined in a range of solvents, k_{ob} being evaluated conveniently by proton NMR line-broadening techniques.[29,43] Solvent-dependent measurements of ΔE_{op} have also been

undertaken for several binuclear ferrocenium-ferrocene ($Cp_2Fe^{+/o}$) complexes, yielding relatively reliable ΔG^*_{os} estimates for the $Cp_2M^{+/o}$ self-exchange reactions.[44]

Figure 2 consists of an illustrative comparison of solvent-dependent optical ΔG^*_{os} values with the corresponding theoretical estimates extracted from Eq(12) in a series of eleven Debye (or near-Debye) polar solvents having known τ_L values. The former values (filled circles) were obtained as noted above for the bis(ferrocenyl)acetylene cation;[44] the latter theoretical estimates (open circles) were calculated as noted in ref. 43a. (See figure caption for further details; note that the optical ΔG^*_{os} values probably contain a small, ca 0.5 kcal mol^{-1}, contribution from inner-shell reorganization.[44]) The plot of $\Delta G^*_{os}/2.3RT$ versus log τ_L^{-1} shown in Fig. 2 (for T = 298K) is suggested by rewriting Eq(8) in the form

$$log\kappa_{el}\nu_n = logk_{ex} - logK_p + \frac{\Delta G^*_{os}}{2.3RT} \qquad (14)$$

where ΔG^*_{is} is assumed to be negligible. This relation indicates that the reliability by which the required solvent-dependent dynamical factor $\kappa_{el}\nu_n$ can be extracted from rate-solvent measurements depends on the relative variations in log ν_n versus $\Delta G^*_{os}/2.3RT$, provided that κ_{el} and K_p remain constant.

Inspection of Fig. 2 reveals several features of interest in this regard. Both the optical and theoretical ΔG^*_{os} values depend systematically on log τ_L^{-1}, so that the rate enhancements expected in dynamically more rapid solvents tend to be partially offset by the occurrence of correspondingly higher activation barriers (larger ΔG^*_{os}). This rough correlation between ΔG^*_{os} and log τ_L^{-1} is commonly observed in polar Debye media. It can be rationalized physically by noting that larger solvent molecules, yielding longer τ_L values, tend to be more

polarizable, thereby also exhibiting larger ϵ_{op} and hence ΔG^*_{os} values when $\epsilon_{op}^{-1} >> \epsilon_o^{-1}$ [Eq(12)]. While the optical ΔG^*_{os} values are typically close to (within ca 0.4 kcal mol^{-1} of) the corresponding theoretical ΔG^*_{os} estimates, Fig. 2 shows that the former values are significantly less dependent on log τ_L^{-1} than are the latter. Possible origins of these small or moderate discrepancies have been discussed in terms of various extant molecular-based models of solvent reorganization; interestingly, the hydrogen-bound solvents water and methanol display the greatest deviations, whereby the optical ΔG^*_{os} values are about 15–25% below the continuum predictions.[44]

These systematic differences between the optical and theoretical ΔG^*_{os} values yield noticeably disparate log ν_n - log τ_L^{-1} dependencies as inferred from the observed rate-solvent behavior depending on whether the correction for the solvent-dependent barriers by means of Eq(14) utilize the optical or theoretical ΔG^* values.[43b] An illustration of the numerical consequences for estimating the solvent-dependent preexponential factor is provided for ferrocenium-ferrocene self exchange in Table II. The barrier-crossing frequencies labelled $\kappa_{el}\nu_n$(op) were obtained from the experimental k_{ex} values and optical barrier heights, ΔG^*_{op}, also given in Table II, by means of Eq(14).[45] (The preequilibrium constant, K_p, was taken to be 0.25 M;[46a] see refs. 29 and 44 for data sources). Listed alongside are corresponding barrier-crossing frequencies, $\kappa_{el}\nu_n$(con), extracted from the k_{ex} values in the same manner but utilizing instead barrier heights, ΔG^*_{con}, estimated by using the dielectric-continuum formula Eq(12). [See ref. 43a for most details; 0.6 kcal mol^{-1} was added to the ΔG^*_{os} values obtained from Eq(12) to allow for the anticipated inner-shell barrier component.[29]] Also listed in Table II are the inverse longitudinal relaxation times, τ_L^{-1}, for each solvent (from ref. 29). (Note that the last two entries, for methanol and propylene carbonate, are given in parentheses since these "non-Debye" solvents exhibit

additional relaxation components at higher frequencies.)

Comparison between the $\kappa_{el}\nu_n$(con) and $\kappa_{el}\nu_n$(op) values for the sequence of solvents in Table II shows that while the former appear to correlate with τ_L^{-1} in the Debye media (albeit with a fractional slope), the latter are approximately *independent of the solvent dynamics*.[43b,45] Quite apart from the anticipated greater *reliability of the* $\kappa_{el}\nu_n$*(op) values*, being based on experimental rather than theoretical barrier estimates, there is good reason to anticipate that the $\kappa_{el}\nu_n$ for $Cp_2Fe^{+/o}$ self exchange is indeed largely independent of the nuclear dynamics. Thus the calculated electronic matrix coupling elements for this reaction are sufficiently small[47] so that largely nonadiabatic pathways are expected to be followed throughout the range of solvent friction encountered in Table II.[39] (Such weak electronic coupling for $Cp_2Fe^{+/o}$ self exchange is also consistent with recent gas-phase rate data.[48]) As noted above [Eq(11)], this circumstance (where $\kappa_{el} << 1$) will yield combined preexponential factors $\kappa_{el}\nu_n$ that approach *independence* of the nuclear component ν_n, in accordance with the observed $\kappa_{el}\nu_n$(op) values. The $\kappa_{el}\nu_n$(op) values are also in most cases markedly smaller than τ_L^{-1}, as expected on the basis of Eq(9) if $\kappa_{el} << 1$.[49] For $Cp_2Co^{+/o}$ and other metallocene self-exchange reactions featuring stronger electronic coupling, however, $\kappa_{el}\nu_n$(op) correlates well with τ_L^{-1} under these conditions, indicating not only that adiabatic pathways are being followed, but the overdamped solvent relaxation model is appropriate under these conditions (see further discussion below).[29,43c]

The systematic observed dependence of the $\kappa_{el}\nu_n$(con) values upon τ_L^{-1} (Table II), on the other hand, would suggest that the reaction is somewhat adiabatic in nature. This, we think false, deduction arises from the systematically greater enhancements in the theoretical compared with the optical ΔG^*_{os} values as τ_L^{-1} increases (Fig. 2), thereby yielding excessively large solvent-dependent barrier

corrections. Consequently, then, the uncritical application of dielectric continuum estimates of ΔG^*_{os} in such solvent dynamical analyses can face difficulties for quantitative purposes.

Nevertheless, it turns out that the use of such theoretical barrier estimates, usually necessitated by the lack of experimental optical data, can yield valuable information on solvent-dynamical effects if used with caution. A useful strategy in analyzing solvent-dependent rate data is to plot log k_{ex} versus the solvent Pekar factor $(\epsilon_{op}^{-1} - \epsilon_o^{-1})$. In view of Eqs(12)-(14):

$$\log k_{ex} = \log \kappa_{el}\nu_n + \log K_p - C(\epsilon_{op}^{-1} - \epsilon_o^{-1}) \qquad (15)$$

where C is a constant which depends in part upon the precursor-state geometry. Despite the inevitable limitations of the dielectric-continuum model in estimating ΔG^*_{os}, evidence from optical data[42] indicates that ΔG^*_{os} in polar media at least correlates approximately with $(\epsilon_{op}^{-1} - \epsilon_o^{-1})$. From Eq(15), then, log k_{ex} should diminish linearly as $(\epsilon_{op}^{-1} - \epsilon_o^{-1})$ increases, provided that $\kappa_{el}\nu_n$ remains largely solvent independent. This behavior has been observed for several homogeneous and electrochemical exchange processes.[51-53] Besides the occurrence of nonadiabatic pathways, such an insensitivity of $\kappa_{el}\nu_n$ to the solvent friction may often be anticipated in the presence of large inner-shell contributions to the barrier-crossing dynamics (see below).

However, in the presence of substantial solvent friction effects, such that $\kappa_{el}\nu_n$ becomes markedly dependent upon τ_L^{-1}, the slope of the log k_{ex} - $(\epsilon_{op}^{-1} - \epsilon_o^{-1})$ plot *can change sign*; since τ_L^{-1} roughly correlates with $(\epsilon_{op}^{-1} - \epsilon_o^{-1})$ (Fig. 2, vide supra) the rate diminutions with increasing Pekar factor can be more than offset by *accompanying* increases in log τ_L^{-1} [Eq(15)]. Consequently, then, the observation of log k_{ex} - $(\epsilon_{op}^{-1} - \epsilon_o^{-1})$ plots having *positive* slopes (albeit with some scatter) can constitute reliable qualitative evidence of the presence of

solvent-friction effects in the reaction dynamics.[46,52]

It is appropriate here to make a few further comments on the limitations of such analyses, especially for more quantitative purposes. First, for several reasons the dielectric-continuum treatment is inherently less reliable in weakly polar or nonpolar media (e.g., chloroform, dichloromethane, dioxane, etc.). The low ϵ_o values (say $\lesssim 15$) that characterize such media lead to greater uncertainties in the applicability of Eqs(12) and (13) due to dielectric saturation and ion-pairing effects.[54] These factors can also yield substantial uncertainties in electrostatic work terms, even for monocharged reactants. An additional difficulty involves electrochemical rate measurements in nonpolar media. Such solvents tend to exhibit low conductances even in the presence of high supporting electrolyte concentrations, exacerbating the acquisition of reliable ET rate data. This problem can be particularly insidious since solvent conductivities (and diffusion coefficients) often correlate crudely with dielectric-friction parameters, so that failure to account properly for the former when evaluating the rate parameters can yield apparent rate-solvent dependencies that infer incorrectly the presence of the latter effect.

While the smaller Pekar factors commonly obtained for nonpolar solvents encourage their use in log k_{ex} - $(\epsilon_{op}^{-1} - \epsilon_o^{-1})$ analyses, such tactics therefore can be problematical. Indeed, some authors have regarded observed deviations from the anticipated negative log k_{ex} - $(\epsilon_{op}^{-1} - \epsilon_o^{-1})$ slopes as signaling breakdowns in the dielectric-continuum formulas themselves rather than to the appearance of solvent dynamical effects.[16c] While we do not agree entirely with this assessment, the desirability of restricting solvent friction analyses to polar media is evident, at least for bimolecular or electrochemical electron-exchange reactions.

Another limitation of dynamical analyses based on relations such as on

Eq(15) is that it is usual to presume (as we have above) that the preequilibrium constant K_p is solvent independent. Aside from the possibility that K_p may contain solvent-specific work terms, for weakly adiabatic processes one anticipates instead that K_p will *diminish systematically* as τ_L^{-1} and hence ν_n increases.[25,29] The reasoning involved can readily be discerned from Eqs(7) and (11). As τ_L^{-1} and hence ν_n increases, κ_{el} for each particular encounter geometry (corresponding to a given H_{12} value) will decrease, thereby shrinking the range of r-dependent geometries that contribute to the bimolecular rate constant [Eq(7)]. The effective K_p will therefore diminish systematically as the nuclear dynamics becomes more rapid. A consequence of this effect, first discussed by Beretan and Onuchic,[55] is that use of the preequilibrium model, whereby K_p is assumed to be solvent-independent, tends to underestimate the effect of solvent-dependent dynamics upon k_{et}.[25] Stated equivalently, the k_{ex}-solvent friction dependencies anticipated by taking into account such spatial integration tend to be noticeably smaller, and of different functionality, than those based on the simple preequilibrium model.[25]

For several of the above reasons, then, the use of multiparametric analyses based on simplified preequilibrium–dielectric continuum models to diagnose and analyze solvent dynamical effects for weakly adiabatic process[56] tend to be, in our opinion, specious rather than genuinely insightful.

IV. Assessment of Solvent-Friction Effects

The foregoing discussion, focussing on the problems of accounting for energetic factors in rate-solvent dynamical analyses, may understandably give the impression that the experimental dissection of such phenomena is fraught with pitfalls. While this is often the case, enough reliable data has now been assembled to allow some broad-based, even quantitative, conclusions to be reached. A number of studies of electrochemical exchange reactions have been

reported in this context, involving inorganic,[52,57] organometallic,[46,58] and organic radical redox couples.[39] In most cases, at least qualitative evidence was obtained for the presence of a solvent-dependent prefactor correlating with τ_L^{-1} in Debye-like media. These results support the notion that the electrochemical reactions are commonly adiabatic, the dynamics being controlled at least partly by overdamped solvent relaxation. An interesting exception is provided by the electron exchange of tris(hexafluoroacetylacetonato)Ru(III)/(II), for which the electrochemical as well as homogeneous-phase kinetics display log k_{ex} – $(\epsilon_{op}^{-1} - \epsilon_o^{-1})$ plots consistent with a solvent-independent prefactor.[51,52] The inferred nonadiabatic behavior can be rationalized on basis of the electronically "insulating" character of the large aliphatic ligands.[52]

In comparison with electrochemical systems, fewer homogeneous self-exchange reactions display clearcut evidence for adiabatic, solvent friction-controlled, dynamics on this basis (eg., see ref. 38c). Nevertheless, the most quantitative dynamical information has been obtained from experimental data of this type. To illustrate, we focus attention further on results obtained in our laboratory for solvent-dependent $Cp_2M^{+/o}$ self exchanges. Unlike the electrochemical exchange reactions, the rates of these processes display an intriguing sensitivity to the metallocene electronic structure as well as the solvent.[29,43] A quantitative analysis of these rate variations, utilizing the optical barrier data noted above, provides insight into the role of donor-acceptor electronic coupling in the overall dynamics.

Figure 3 summarizes some key experimental data of this type, taken from ref. 29, in the form of a plot of log k'_{ex} for five $Cp_2M^{+/o}$ couples in eleven Debye (or near-Debye) solvents, against log τ_L^{-1}. The "barrier-corrected" rate constants k'_{ex} [referring to a fixed (cusp) barrier height of 5.0 kcal mol^{-1}] were obtained from the measured k_{ex} values by correcting them for the solvent-

dependent ΔG^{*}_{os} values (which range from ca 4.6 to 5.4 kcal mol^{-1}). The remaining solvent-induced rate variations should largely reflect changes in dynamics rather than energetics. Inspection of Fig. 2 shows that the log k'_{ex} - log τ_L^{-1} dependencies depend markedly on the metallocene couple. While k'_{ex} for the least facile, $Cp_2Fe^{+/o}$, reactants exhibit little dependence on τ_L^{-1}, the log k'_{ex} - log τ_L^{-1} slopes increase progressively for the more rapid $Cp_2Co^{+/o}$ systems as k'_{ex} in a given solvent increases. In a given solvent, the k_{ex} values vary by up to 100 fold. In addition, although there is significant scatter, the log k'_{ex} - log τ_L^{-1} slopes for a given reaction tend to decrease towards larger log τ_L^{-1} values.

These observations are in harmony with expectations based on a consideration of variable donor-acceptor electronic coupling. For this purpose, Fig. 4 displays theoretical log k'_{ex} - log τ_L^{-1} plots (also taken from ref. 29) computed for the same set of solvents as in Fig. 3, for spherical reactants featuring the sequence of electronic coupling matrix elements, H^{o}_{12} (referring to reactant contact), as indicated. The k'_{ex}(calc) values were calculated from conventional solvent-dynamical theory, taking into account both barrier-top shape effects and a spatial integration of bimolecular encounter geometries by using Eq(7). The form of these log k'_{ex}(calc) - log τ_L^{-1} plots in Fig. 4, closely similar to the experimental curves (Fig. 3), can readily be understood in terms of Eq(11). Thus enlarging H_{12} and/or τ_L will increase κ_{el} and hence the degree to which solvent dynamics, rather than nonadiabatic electron tunneling, controls the barrier-crossing frequency, as seen by the systematic increases in the log $'_{ex}$(calc) - log τ_L^{-1} slopes under these conditions (Fig. 4). [The scatter seen in Fig. 4 for some low-friction solvents arises from the variable anticipated effects of solvent inertia, corresponding to the emergence of the TST limit (vide supra).[29]]

Significantly, Fig. 4 shows that the appearance of substantial solvent friction effects requires the presence of relatively strong electronic coupling

($H_{12}^{o} \gtrsim 0.2$ kcal mol^{-1}) for the range of τ_L^{-1} values, ca 10^{11} to 4 x 10^{12} s^{-1}, that characterize most polar Debye media at ambient temperatures. Further, the log k'_{ex}(calc) - log τ_L^{-1} slopes are significantly below unity even at the highest H_{12} and τ_L values encountered in Fig. 4. This latter feature arises from the expectation of friction-dependent K_p values, as noted above. Intercomparisons between Figs. 3 and 4 enable approximate estimates of H_{12}^{o} for the various metallocene self-exchange reactions to be obtained. These vary from about 0.1 kcal mol^{-1} for $Cp_2Fe^{+/o}$ to 0.5 kcal mol^{-1} for $Cp_2Co^{+/o}$ and 1.0 kcal mol^{-1} for $Cp'_2Co^{+/o}$ (Cp' = pentamethylcyclopentadienyl). Interestingly, the first two experimental H_{12}^{o} estimates are in approximate accord with the average values obtained for various metallocenium-metallocene precursor geometries by Newton et al.[47] The greater electronic coupling for the cobalt versus the iron metallocenes can be understood qualitatively in terms of the ligand- and metal-centered nature, respectively, of the molecular orbitals that participate in electron transfer.[42,47]

Overall, these and other experimental results indicate that overdamped solvent relaxation as described in Debye media by τ_L^{-1} can provide at least an approximate description of the nuclear barrier-crossing dynamics, even though substantial donor-acceptor electronic coupling is required in order to yield a dominant influence of solvent friction upon the reaction rate. The findings, however, certainly do not exclude the occurrence of significant deviations from the simple dielectric continuum picture associated with short-range solvent reorganization and other factors.

V. Influence of Rapid Solvent Relaxation Components

Given this largely satisfactory picture, it is of particular interest to explore the manner and extent to which the presence of additional, more rapid, overdamped relaxation components may influence the barrier-crossing dynamics.

At least the qualitative presence of such effects has been diagnosed in several cases, especially for primary alcohols, from the markedly ($\gtrsim$ 10 fold) higher k_{ex} values obtained for both organic[39d] and organometallic redox couples[30,43a,46b,61] in such alcohols in comparison with the rates in aprotic media yielding similar anticipated barriers. As mentioned above, primary alcohols contain significant dispersion components of the dielectric loss spectra at markedly ($\gtrsim$ 10 fold) higher frequencies than the major "Debye" relaxation.[31] However, the use of analyses employing dielectric-continuum ΔG^*_{os} estimates may well over- estimate the importance of such effects, as adjudged by the markedly (ca 0.5–1 kcal mol^{-1}) smaller ΔG^*_{os} values obtained for such hydrogen-bound solvents from optical data.[44]

Of particular interest is the comparison between the direct information on rapid solvent relaxation components obtained recently from subpicosecond TDFS measurements[18a,34] with data for adiabatic barrier-crossing dynamics in activated ET. Pertinent data extracted from the sole comparison along these lines reported so far[61] are summarized in Table III (taken from ref. 20). The two far right-hand columns contain net barrier-crossing frequencies, $\kappa_{el}\nu_n$, in eight selected solvents extracted for a pair of metallocene self-exchange reactions from k_{ex} and optical ΔG^*_{os} data using the same procedure as in Table II. The redox couples, labelled $Cp^*_2Co^{+/o}$ (Cp^* = carboxymethyl-cyclopentadienyl) and $HMFc^{+/o}$[(hydroxymethyl)ferrocenium-ferrocene] are selected since they display largely adiabatic and nonadiabatic behavior, respectively,[29] and can be examined in a range of solvents, including water.[43c]

Alongside these barrier-crossing frequencies are listed inverse relaxation times, τ_s, for each solvent obtained from TDFS data for coumarin probes by Barbara et al.[34,61] Almost all these solvents display nonexponential decay behavior; the relaxation times and weighting factors resulting from biexponential

fits are given in Table III, along with corresponding τ_L^{-1} values extracted from dielectric loss spectra. For the most part, the "longer-time" τ_s^{-1} components are comparable (within ca twofold of) the corresponding τ_L^{-1} values. Two of the solvents, propylene carbonate and methanol, exhibit discernable "shorter-time" dielectric-loss components; the predominant "long-time" τ_L^{-1} values are given in parentheses in Table III.

Similarly to $Cp_2Fe^{+/o}$ self exchange (Table II, vide supra), the $\kappa_{el}\nu_n$ values for $HMFe^{+/o}$ are uniformly smaller than τ_L^{-1} or τ_s^{-1}, and are insensitive to the solvent dynamics, as expected for a nonadiabatic process. For $Cp^*_2Co^{+/o}$, however, the $\kappa_{el}\nu_n$ values not only correlate well with the solvent relaxation dynamics, but are also uniformly close to (within 1.5 fold of) the *faster* τ_s^{-1} component (Table III). Admittedly, this agreement between the *absolute* $\kappa_{el}\nu_n$ and τ_s^{-1} values is probably fortuitous given the inevitable uncertainties in extracting the former. The observed close correlation nevertheless demonstrates the importance of the more rapid dynamical component in accelerating the ET barrier-crossing frequency. The findings for methanol and water are perhaps of greatest interest.[43c,61] The influence of the high-frequency relaxation in methanol is especially striking, yielding barrier-crossing frequencies that approach those in water and other low-friction media despite the presence of a markedly (10-30) longer τ_L value. Comparable findings have been obtained for other adiabatic metallocene reactions.[29,30,43] Despite these substantial rate accelerations, all the inferred $\kappa_{el}\nu_n$ values are still significantly smaller than would correspond to the anticipated inertial (i.e., TST) limit, as can be gauged by comparing the $\kappa_{el}\nu_n$ values with the ω_o estimates in Table I.

The issue of the degree to which such rapid overdamped relaxations can enhance ET rates has been the subject of substantial theoretical interest (see ref. 30).[8c,10a,14a,b,62] In particular, a treatment by Hynes,[8c] which considers

dynamical effects in both reactant well and barrier-top regions, yields predictions largely in accord with these experimental observations: even relatively small amplitude rapid relaxations can yield substantial rate accelerations.[30,61] This deduction, based on analytic theory, is also in harmony with the results of numerical simulations utilizing a cusp barrier.[63] The degree to which the rapid dynamical components accelerate ν_n is predicted to diminish somewhat as the donor-acceptor coupling (H_{12}) increases, so that the barrier top becomes more "rounded".[8c,30] This effect arises from the increased influence that overdamped relaxation in the barrier-top region, rather than in the wells, is expected to exert under these conditions. Nevertheless, numerical calculations suggest that the accelerating role of higher-frequency relaxations remains marked even at large H_{12} values, around 1 kcal mol^{-1}.[30] Dipole *translation*, as well as rotational, motion is also predicted to contribute to the rapidity of the TDFS and barrier-crossing dynamics in methanol.[8b,61]

The common presence of very rapid (say $\tau_s \lesssim 0.1$ps), overdamped relaxation even in supposedly "Debye" media, has also been suggested by several recent molecular dynamical (MD) simulations.[19a] Besides the numerical value of such calculations, they can provide interesting insight into the physical origins of solvent relaxation. So far, most solvents examined (eg., water, acetonitrile) constitute relatively low-friction media, where the role of solvent inertia is relatively important in the overall dynamics.[19a] It would clearly be of substantial interest to pursue MD simulations for solvents where overdamped relaxation is anticipated to be more dominant.

VI. Influence of Reactant Intramolecular Dynamics

Up to this point, we have considered dynamical solvent effects for experimental ET systems where the activation barrier is known (or believed) to arise wholly or predominantly from dipolar solvent reorganization. A much more

common circumstance, however, involves the presence of barrier components from reactant intramolecular (inner-shell) reorganization that are comparable to, or larger than, the solvent contribution. Given that the frequencies of such intramolecular motions, especially vibrational modes, are usually anticipated to be higher than for solvent overdamped or even inertial motion, one might anticipate that the barrier-crossing frequency would commonly be dominated by inner-shell rather than solvation dynamics. As mentioned above, this conclusion indeed commonly applies in the TST limit, as prescribed by Eq(2). A rather different situation might be anticipated in the presence of solvent friction: even though the presence of higher-frequency inner-shell distortions should accelerate barrier passage, the reaction rate may be limited in part by a slow diffusive approach to the barrier top. Despite its practical importance, relatively little attention has been devoted to this issue. Nevertheless, a detailed theoretical treatment for cusp barriers, and spanning the range from activationless to activated ET processes, has been outlined by Marcus and coworkers.[9]

Some numerical consequences of their treatment for activated ET processes are illustrated in Fig. 5. This consists of a plot of log k_{ex} for a model electron-exchange reaction[64] versus the inner-shell barrier ΔG^{*}_{is}, with the outer-shell barrier held at 4.0 kcal mol^{-1}. Both sets of curves shown refer to a quartet of τ_L^{-1} values, varying from 6 x 10^{10} to 6 x 10^{12} s^{-1} (the lowest and highest traces, respectively); these values were chosen so to span the commonly encountered dynamical range. The quartet of solid curves refer to an inner-shell (vibrational) frequency, ν_{is}, of 5 x 10^{13} s^{-1}, whereas the corresponding dashed curves were computed for a tenfold smaller frequency. The rates were computed for a tenfold smaller frequency. The rates were computed chiefly in the manner prescribed by Marcus et al[9]; full details will be provided elsewhere.[64]

Physically, the dynamical effect of the inner-shell component arises from the provision of additional channels by which the reaction can be consumated once the vicinity of the barrier top is reached. In the absence of such a vibrational reaction coordinate, electron transfer occurs only when the system reaches the barrier cusp entirely by diffusive solvent motion. In the calculations shown in Fig. 5, the reaction is considered to be consummated under these latter conditions at the barrier cusp by means of solvent inertial motion (ω_o is taken to be 10 ps^{-1}); this feature yields a self-consistent kinetic treatment in the absence and presence of the vibrational reaction coordinate.[65]

Examination of Fig. 5 reveals several significant features. The inclusion of the inner-shell barrier component initially *increases* the rate constant, even though decreases are seen eventually for moderate ($\gtrsim$ 0.5–1 kcal mol^{-1}) ΔG^*_{is} values. The former effect is due to the occurrence of an increasingly rapid barrier-crossing frequency, arising from the inclusion of the inner-shell dynamics, *offsetting* the influence of the larger activation barrier. At a given ν_{is}, the vertical displacement of the various traces shows the sensitivity of the reaction rate to τ_L^{-1}. As might be expected, this sensitivity decreases progressively as ΔG^*_{is} becomes larger, corresponding to an increasing dominance by the inner-shell dynamics under these conditions. Nevertheless, it is interesting to note that a significant or even substantial dependence of log k_{ex} upon log τ_L^{-1} can remain in the presence of the inner-shell barrier. This is especially the case in the presence of *more rapid* inner-shell dynamics (see the solid versus the dashed traces in Fig. 5).

This last property, where the influence of varying solvent friction upon ν_n becomes more pronounced as the overdamped dynamics become *slower*, is in complete contrast to the TST picture. A qualitatively similar prediction can also be deduced[46a] from an earlier theoretical treatment by Ovchinnikova.[66]

Moreover, nuclear tunneling can diminish the influence of high-frequency vibrations (say, $\nu_{is} \gtrsim 1 \times 10^{13}\ s^{-1}$), enhancing the predicted effects of solvent friction upon k_{ex} even at ambient temperatures. Consequently, then, there are theoretical reasons to anticipate that the barrier-crossing dynamics can be influenced significantly by overdamped solvent motion even in the presence of much more rapid inner-shell barrier components, although the former effects should be largely attenuated when $\Delta G^*_{is} \gtrsim \Delta G^*_{os}$.

Experimental tests of such theoretical predictions for activated ET are so far surprisingly sparse. One contributing factor is that there is a paucity of suitable outer-sphere reactant systems, especially having low charges so to minimize electrostatic work terms, for which the inner-shell barriers are known, and preferably variable by suitable chemical modification. One such study for the solvent-dependent electrochemical exchange of cobalt clathrochalates has indicated that significant solvent friction effects can be maintained even when $\Delta G^*_{is} \sim \Delta G^*_{os}$.[57] Some further evidence that the theoretical predictions such as in Fig. 5 may overestimate the influence of inner-shell vibrations in muting solvent-friction effects has also been obtained from a recent examination of electrochemical and self-exchange kinetics for various sesquibicyclic hydrazines.[67] One limitation of the theoretical treatment noted above[9] is that it does not consider the effects of barrier-top roundedness arising from electronic coupling. Similarly to the discussion above, the inevitable presence of this factor is anticipated to enhance the role of solvent friction in mediating the influence of additional vibrational reaction channels upon ν_n.

VII. Activation-Parameter Analyses

As already mentioned, at first sight the evaluation of activation parameters, i.e., temperature-dependent rate measurements, would appear to be a valuable tactic for extracting information on ET barrier-crossing dynamics. At

least in principle, the Arrhenius preexponential factor, A_{et}, obtained conventionally from the intercept of $\ln k_{ex} - T^{-1}$ plots, should be related closely to the desired frequency factor $\kappa_{el}\nu_n$. The approach has indeed been utilized on a number of occasions with this objective in mind.[38f,43a,46a] Although yielding useful information, at least for bimolecular processes this procedure suffers from some ambiguities that conspire to render it less useful for assessing $\kappa_{el}\nu_n$.

First, the measured activation enthalpy, and hence the inferred preexponential factor, are expected to be affected by the enthalpic and entropic contributions to the free energy of precursor-complex formation. Such components may well be sensitive to the local solvation and other intermolecular interactions in the precursor state versus the separated reactants to a greater extent than the overall free energy, and hence K_p.[68] Even for reactions involving monocharged cation/neutral pairs, such as the metallocene self exchanges considered above, unexpectedly low Arrhenius preexponential factors, A_{pe}, are obtained that may reflect in part unfavorable entropic contributions to the precursor-complex stability.[43a]

A second complication concerns the anticipated temperature dependence of the barrier-crossing frequency $\kappa_{el}\nu_n$. While the usual Arrhenius treatment tacitly assumes that the overall preexponential factor A_{pe} is temperature independent, this is seldom expected to be the case, especially for barrier crossing controlled by solvent friction. Thus τ_L^{-1}, and hence ν_n, is expected to increase with temperature, thereby yielding inferred A_{pe} values that are larger than $K_p\kappa_{el}\nu_n$.[43a,46a] While this factor can be taken into account in activation-parameter analyses,[43a,46a] such procedures are obliged to rely on the presumed validity of the combined Debye/dielectric continuum or other treatments in accounting for the temperature dependence of the dynamics. Given the likely quantitative limitations of the theoretical treatments noted above, the procedure

is susceptible to difficulties.

Nonetheless, under favorable circumstances, such as the examination of rate parameters for related sequences of reactions, the evaluation of activation-parameter data may have considerable virtues for the elucidation of dynamical effects. Indeed, this tactic has been utilized in several solvent dynamical studies, mostly involving small-barrier ET processes.[69] Most importantly, the approach has greatest merit for the examination of intramolecular electron-transfer systems, where the difficulties associated with the energetics of precursor-complex formation are absent.[70]

VIII. Some Expectations and Unresolved Issues: When Do Solvent-Friction Effects Matter?

In some respects, our current understanding of dynamical solvent effects in activated ET processes might be deemed satisfactory. While many quantitative (and important) details are lacking, there is widespread evidence available from solvent-dependent electron-exchange studies of the importance of overdamped solvent relaxation to the reaction dynamics. An initial quantitative link has been made with the real-time dynamical information obtainable from TDFS measurements, and the rough applicability of continuum-Debye descriptions of solvent dynamics established, along with the likely importance of rapid overdamped components, in some cases. The central role of donor-acceptor electronic coupling in mediating the occurrence, as well as the characteristics, of such nuclear dynamical effects has also become apparent on an experimental as well as theoretical basis.

There are some reasons, however, to suspect that this scenario may be overly optimistic or perhaps even misleading. First, our understanding of the type and range of activated ET processes susceptible to dynamical solvent effects is discomfortingly inadequate. This situation is related to a lack of reliable

independent information on electronic coupling, especially for electrochemical reactions. The extent of solvent dynamical effects often observed for such processes[38,39] infer that substantial electronic coupling, $H_{12} \gtrsim 0.5$ kcal mol^{-1}, is commonly present. While there is some theoretical justification for the presence of such electronic coupling for reactions at metal surfaces,[71] the broadbased occurrence of adiabatic pathways for outer-sphere reactions, as inferred from the rate-solvent behavior, would be surprising.

Unfortunately, a large fraction of the electrochemical reactions amenable to such solvent-dependent analysis exhibit k_{ex} values (ca 0.1–10 cm s^{-1}) that approach (or even surpass?) the limit that can be evaluated reliably even by contemporary kinetic techniques, such as a.c. impedance and/or microelectrode-based approaches. As mentioned above, this problem can be particularly insidious since the resulting systematic errors in the rate data have a solvent-dependent character which is similar to that expected in the presence of solvent dynamical effects. Given the additional uncertainties associated with the usage of dielectric continuum estimates of ΔG^{*}_{os} to electrochemical systems, there are good reasons to be wary of some dynamical analyses undertaken for electrochemical systems. Related difficulties can also hamper analyses for some homogeneous-phase reactions. For example, very rapid self-exchange reactions, having rates approaching the bimolecular diffusion limit, are expected can yield solvent-dependent rate behavior reminiscent of dynamical solvent relaxation merely as a result of viscosity-dependent solute transport effects.[38a]

Another significant unresolved issue, again associated with electronic-coupling effects, concerns the likely importance of solvent relaxation within the reactant (and product) free-energy wells versus that in the barrier-top region. For cusp barriers, featured in the original Zusman model[6] [leading to Eq(9)] as well as numerous subsequent theoretical treatments, the former component is

necessarily dominant. However, this dynamical model is inherently somewhat artificial since cusp barriers arise from the circumstance $H_{12} \rightarrow 0$, where electron tunneling rather than nuclear dynamics will actually control the net barrier-crossing frequency. Recent MD simulations performed for a "model aprotic" solvent involving moderate and large electronic coupling (H_{12} = 1 and 5 kcal mol^{-1}, respectively) yielded little evidence of any solvent friction in the former case, and mild friction arising from overdamped motion only in the barrier-top region in the latter circumstance.[17,72] The solvent model employed in these studies appears to exhibit only low-friction characteristics. Nevertheless, it is disquieting to note that there is apparently no evidence so far from MD simulations for the occurrence of ET solvent friction associated with well relaxation, the observed rate diminutions being associated only with recrossings within the barrier-top region.[17,72]

As already noted, there is good reason to expect overdamped motion in the barrier-top versus the well regions to become a more prevalent contributor to ν_n as the electronic coupling increases, and hence the effective "barrier-top frequency", ω_b, decreases to the extent that it becomes comparable to the well frequency, ω_o.[8c,30] Given the general requirement that at least moderate electronic coupling be present to engender nuclear-dynamical control, it is conceivable that the solvent friction observed experimentally for activated ET processes arises merely from relaxation within the barrier-top region. This circumstance would of course be aided by reaction pathways that utilize preferentially reaction geometries having especially large electronic couplings. Such a circumstance is plausible, for example, for $Cp_2Co^{+/o}$ self exchange where one specific (D_{5h}) internuclear geometry is predicted to yield especially strong coupling, $H_{12} \simeq 2.5$ kcal mol^{-1}.[47,73] Further MD simulations, however, preferably for realistic overdamped model solvents, are required to resolve this important

question.

A general limitation of experimental studies so far is that the range of ET reaction types explored is relatively narrow, being restricted almost entirely to outer-sphere electron-exchange processes. It would be desirable, for example, to examine exoergic processes, such as homogeneous-phase cross reactions, in this context. Similar analyses could be undertaken as outlined above, although it is necessary to correct the observed solvent-dependent rates for variations in the thermodynamic driving-force contribution to ΔG^* present for cross reactions. At least one study along these lines has recently been reported.[76] Especially given the central influence of electronic coupling in solvent dynamics, it would be of particular interest to examine inner-sphere ET and other "strong-overlap" charge-transfer reactions. Despite the extensive theoretical and computational work on some aspects of strong-overlap charge-transfer processes,[77] related solvent-dependent experimental studies are rare. An interesting recent example, however, concerns the evaluation of primary kinetic isotope effects (k_H/k_D) for hydride transfer.[78] A significant solvent dependence of k_H/k_D was observed, from a maximum of ca 5-5.5 in low-friction media to ca 3.0 in some other solvents. Although a quantitative relationship between k_H/k_D and solvent friction was not established, the results are roughly consistent with a shift from near-complete rate control by hydride tunneling to partial control by overdamped solvent dynamics.[78] This interpretation is closely analogous to the phenomenon of solvent friction-dependent adiabaticity for electron transfer, embodied in Figs. 3 and 4.

Most importantly, it would be desirable to explore the kinetics of unimolecular, preferably rigid intramolecular, ET processes with regard to solvent dynamical effects. Compared with bimolecular (and electrochemical) processes, such systems have the major virtue of eliminating uncertainties

regarding the energetics and geometries of precursor-complex formation. Although a number of photoexcited intramolecular ET reactions have been examined,[18] as mentioned above, these apparently feature small or negligible ($\lesssim k_BT$) barriers; few such studies involving *activated* intramolecular ET process have been reported so far. Although there are experimental difficulties to be overcome, there are good reasons to emphasize intramolecular ET processes in future studies. It will be desirable to identify reactant systems for which both optical ET energetics and thermal ET rates can be obtained, thereby enabling reliable separations between dynamical and energetic factors to be achieved. The evaluation of activation parameters should also prove to be valuable in this regard, the complications of the precursor-formation energetics that plague their interpretation for intermolecular systems being absent. Such systems should also be useful for expanding experimental inquiries of dynamical effects into a wider range of solvating media, such as polymers[76] and glasses.

Overall, then, there is some reason to be optimistic that our understanding of solvent-friction, as for other dynamical, aspects of ET reaction kinetics will be placed on an increasingly firm experimental basis in the future. Such studies, especially in conjunction with MD simulations and electronic structural calculations, should lead to a deeper understanding of some of these fascinating mysteries surrounding solvent and related environmental effects in charge-transfer processes.

ACKNOWLEDGMENTS

The continued financial support of our research on this topic by the Office of Naval Research is gratefully acknowledged. I am thankful for the industrious efforts of my coworkers in this area since 1984 - Roger Nielson, Alex Gochev, Neal Golovin, Tom Gennett, Don Phelps, and especially the late George McManis. I remain indebted to George, in particular, for sharing with me a wondrous sense of excitement (and sheer fun), as well as fulfillment, in exploring this enticing area of physical chemistry.

REFERENCES AND NOTES

1. (a) Marcus, R.A., J. Chem. Phys., **1956**, 24, 966; 979; (b) Marcus, R.A., J. Chem. Phys., **1965**, 43, 679; (c) Marcus, R.A., Ann. Rev. Phys. Chem., **1964**, 15, 155

2. For overviews of electron-transfer models within the framework of the TST treatment, see (a) Sutin, N.; Acc. Chem. Res., **1982**, 15, 275; (b) Sutin, N., Prog. Inorg. Chem., **1983**, 30, 441

3. Explanation broadbased reviews include: (a) Hynes, J.T., in "The Theory of Chemical Reactions," Baer, M., ed, CRC Press, Boca Raton, FL, 1985, Vol. 4, p.171; (b) Hynes, J.T., J. Stat. Phys., **1986**, 42, 149; (c) Chandler, D., J. Stat. Phys., **1986**, 42, 49

4. McManis, G.E.; Gochev, A.; Weaver, M.J., Chem. Phys., **1991**, 152, 107, and references cited therein.

5. Kramers, H.A., Physica, **1940**, 7, 284.

6. Zusman, L.D., Chem. Phys., **1980**, 49, 295.

7. (a) Calef, D.F.; Wolynes, P.G., J. Phys. Chem., **1983**, 87, 3387; (b) Wolynes, P.G., J. Chem. Phys., **1987**, 86, 5133.

8. (a) van der Zwan, G.; Hynes, J.T., J. Chem. Phys., **1982**, 76, 2993; (b) van der Zwan, G.; Hynes, J.T., Chem. Phys. Lett., **1983**, 101, 367; (c) Hynes, J.T., J. Phys. Chem., **1986**, 90, 3701; van der Zwan, G.; Hynes, J.T., Chem. Phys., **1991**, 152, 169.

9. (a) Sumi, H.; Marcus, R.A., J. Chem. Phys., **1986**, 84, 4894; (b) Nadler, W.; Marcus, R.A., J. Chem. Phys., **1987**, 86, 3906

10. (a) Rips, I.; Jortner, J., J. Chem. Phys., **1987**, 87, 2090; (b) Rips, I.; Klafter, J.; Jortner, J., J. Chem. Phys., **1988**, 89, 4288

11. Belousov, A.A.; Kuznetsov, A.M.; Ulstrup, J., Chem. Phys., **1989**, 129, 311

12. Newton, M.D.; Friedman, H.L., J. Chem. Phys., **1988**, 88, 4460

13. (a) Morillo, M.; Cukier, R.I., J. Chem. Phys., **1988**, 89, 6736; (b) Yang, D.Y.; Cukier, R.I., J. Chem. Phys., **1989**, 91, 281

14. (a) Sparpaglione, M.; Mukamel, S., J. Phys. Chem., **1987**, 91, 3938; (b) Sparpaglione, M.; Mukamel, S., J. Chem. Phys., **1988**, 88, 1465;

(c) Yau, Y.J.; Sparpaglione, M.; Mukamel, S., J. Phys. Chem., 1988, 92, 4842

15. (a) Bagchi, B.; Chandra, A.; Fleming, G.R., J. Phys. Chem., 1990, 94, 5197; (b) Chandra, A.; Bagchi, B., J. Phys. Chem., 1989, 93, 6996.

16. For reviews of analytic theory, see: (a) Onuchic, J.N.; Wolynes, P.G., J. Phys. Chem., 1988, 92, 6495; (b) Bagchi, B., Ann. Rev. Phys. Chem., 1989, 40, 115; (c) Kuznetsov, A.M.; Ulstrup, J.; Vorotyntsev, M.A., in "Chemical Physics of Solvation," Part C, Dogonadze, R.R.; Kalman, E.; Kornyshev, A.A.; Ulstrup, J., eds, Elsevier, Amsterdam, 1988, Chapter 3; (d) Mukamel, S.; Yan, Y.T., Acc. Chem. Res., 1989, 22, 301.

17. (a) Zichi, D.A.; Ciccotti, G.; Hynes, J.T.; Ferrario, M., J. Phys. Chem., 1989, 93, 6261; (b) Bader, J.S.; Kuharski, R.A.; Chandler, D., J. Chem. Phys., 1990, 93, 230.

18. For overviews, see: (a) Barbara, P.F.; Jarzeba, W., Adv. Photochem., 1990, 15, 1; (b) Bagchi, B.; Fleming, G.R., J. Phys. Chem., 1990, 94, 9; (c) Simon, J.D., Pure Appl. Chem., 1990, 62, 2243

19. For overviews, see: (a) Maroncelli, M., J. Mol. Liquids, in press; (b) Maroncelli, M.; MacInnis, J.; Fleming, G.R., Science, 1989, 243, 1674; (c) Simon, J.D., Acc. Chem. Res., 1988, 21, 128

20. Weaver, M.J.; McManis, G.E., Acc. Chem. Res., 1990, 23, 294

21. Hynes, J.T., article in present Chem. Revs. issue

22. Hupp, J.T.; Weaver, M.J., J. Electroanal. Chem., 1983, 152, 1.

23. The usual units of K_p, M and cm, for homogeneous and electrochemical reaction, respectively, account for the usual k_{ob} units, M^{-1} s^{-1} and cm s^{-1}, given that k_{et} is a unimolecular rate constant for reaction within a given precursor geometry.

24. (a) Tembe, B.L.; Friedman, H.L.; Newton, M.D., J. Chem. Phys., 1982, 76, 1490; (b) Newton, M.D.; Sutin, N., Ann. Rev. Phys. Chem., 1984, 35, 437

25. Gochev, A.; McManis, G.E.; Weaver, M.J., J. Chem. Phys., 1989, 91, 906

26. Note that the oft-quoted Eq(9) is a special case of relationships given in refs. 6 and 7a (and elsewhere) when $\Delta G^\circ = 0$.

27. For reviews of the interpretation of dielectric loss spectra, see: (a) Hill, N.E.; Vaughan, W.E.; Price, A.H.; Davis, M., "Dielectric Properties and Molecular Behavior," Van Nostrand Reinhold, London, 1969; (b) Böttcher, C.J.F.; Bordewijk, P., "Theory of Electric Polarization," Elsevier, Amsterdam, 1978.

28. For an erudite discussion of the meaning of τ_L in relation to τ_D, see: Kivelson, D.; Friedman, H., J. Phys. Chem., 1989, 93, 7026

29. McManis, G.E.; Nielson, R.M.; Gochev, A.; Weaver, M.J., J. Am. Chem. Soc., 1989, 111, 5533

30. McManis, G.E.; Weaver, M.J., J. Chem. Phys., 1989, 90, 912

31. For example, see: (a) Garg, S.K.; Symth, C.P., J. Phys. Chem., 1965, 69, 1294; (b) Crossley, J., Adv. Mol. Relax. Processes, 1970, 2, 69

32. Onsager, L., Can. J. Chem., 1977, 55, 1819

33. (a) Maroncelli, M.; Fleming, G.R., J. Chem. Phys., 1987, 86, 6221; but see erratum in: J. Chem. Phys. 1990, 92, 3251; (b) Maroncelli, M.; Fleming, G.R., J. Chem. Phys., 1988, 89, 875.

34. (a) Kahlow, M.A.; Jarzeba, W.T.; Kang, T.J.; Barbara, P.F., J. Chem. Phys., 1989, 90, 151; (b) Jarzeba, W.; Walker, G.C.; Johnson, A.E.; Barbara, P.F., Chem. Phys., 1991, 152, 57.

35. (a) Chandra, A.; Bagchi, B., J. Chem. Phys., 1989, 90, 7338; (b) Chandra, A.; Bagchi, B., J. Phys. Chem., 1989, 93, 6996

36. Kornyshev, A.A.; Kuznetsov, A.M.; Phelps, D.K.; Weaver, M.J., J. Chem. Phys., 1989, 91, 7159

37. McManis, G.E.; Mishra, A.K.; Weaver, M.J., J. Chem. Phys., 1987, 86, 5550

38. (a) Harrer, W.; Grampp, G.; Jaenicke, W., Chem. Phys. Lett., 1984, 112, 263; (b) Harrer, W.; Grampp, G.; Jaenicke, W., J. Electroanal. Chem., 1986, 209, 223; (c) Kapturkiewicz, A.; Jaenicke, W., J. Chem. Soc. Farad. Trans. 1, 1987, 83, 2727; (d) Grampp, G.; Harrer, W.; Jaenicke, J. Chem. Soc. Farad. Trans. 1, 1987, 83, 161; (e) Grampp, G.; Harrer, W.; Jaenicke, W., J. Chem. Soc. Farad. Trans. 1, 1988, 84, 366; (f) Grampp, G.; Kapturkiewicz, A.; Jaenicke, W., Ber. Bunseng. Phys. Chem., 1990, 94, 439

39. (a) Kapturkiewicz, A.; Behr, B., J. Electroanal. Chem., 1984, 179, 184;

(b) Kapturkiewicz, A.; Opallo, M., J. Electroanal. Chem., **1985**, 185, 15; (c) Kapturkiewicz, A., Electrochim. Acta., **1985**, 30, 1301; (d) Opallo, M., J. Chem. Soc. Farad. Trans. 1, **1986**, 82, 339

40. (a) Dzhavakhidze, P.G.; Kornyshev, A.A.; Krishtalik, L.I., J. Electroanal. Chem., **1987**, 228, 329; (b) Phelps, D.K.; Kornyshev, A.A.; Weaver, M.J., J. Phys. Chem., **1990**, 94, 1454

41. For an explanative review, see: Creutz, C., Prog.Inorg.Chem., **1983**, 30, 1

42. Nielson, R.M.; Golovin, M.N.; McManis, G.E.; Weaver, M.J , J. Am. Chem. Soc., **1988**, 110, 1745

43. (a) Neilson, R.M.; McManis, G.E.; Golovin, M.N.; Weaver, M.J., J. Phys. Chem., **1988**, 92, 3441; (b) Nielson, R.M.; McManis, G.E.; Safford, L.K.; Weaver, M.J., J. Phys. Chem., **1989**, 93, 2152; (c) Nielson, R.M.; McManis, G.E.; Weaver, M.J., J. Phys. Chem., **1989**, 93, 4703

44. McManis, G.E.; Gochev, A.; Nielson, R.M.; Weaver, M.J., J. Phys. Chem., **1989**, 93, 7733

45. (a) Note that the solvent-dependent rate constants for $Cp_2Fe^{+/o}$ self exchange listed in Table I, taken from refs. 29 and 43b, differ significantly from earlier published values[45b]; as discussed in ref. 43b the latter values suffer from systematic errors in the NMR line-broadening analysis; (b) Yang, E.S.; Chan, M.-S.; Wahl, A.C., J. Phys. Chem., 1980, 84, 3094

46. (a) Gennett, T.; Milner, D.F.; Weaver, M.J., J. Phys. Chem., **1985**, 89, 2787; (b) McManis, G.E.; Golovin, M.N.; Weaver, M.J., J. Phys. Chem., **1986**, 90, 6563

47. Newton, M.D.; Ohta, K.; Zhang, E., J. Phys. Chem., **1991**, 95, 2317

48. Phelps, D.K.; Gord, J.R.; Freiser, B.S.; Weaver, M.J., J. Phys. Chem., **1991**, 95, 4338

49. The recognition that κ_{el}, and hence $\kappa_{el}K_p$, will depend inherently on ν_n for weakly adiabatic as well as nonadiabatic processes has not always been made in the recent literature (for example, see ref. 50).

50. Fawcett, W.R.; Foss, C.A., J. Electroanal. Chem., **1988**, 252, 221

51. Chan, M.-S.; Wahl, A.C., J. Phys. Chem., **1982**, 86, 126

52. Weaver, M.J.; Phelps, D.K.; Nielson, R.M.; Golovin, M.N.; McManis, G.E., J. Phys. Chem., 1990, 94, 2949

53. For example: (a) Brandon, J.R.; Dorfman, L.M., J. Chem. Phys., 1970, 53, 3849; (b) Li T.T-T.; Brubaker, C.H., Jr., J. Organomet. Chem., 1981, 216, 223

54. An examination of these effects utilizing optical electron-transfer energies is described in: (a) Blackburn, R.L.; Hupp, J.T., Chem. Phys. Lett., 1988, 150, 399; (b) Blackburn, R.L.; Hupp, J.T., J. Phys. Chem., 1990, 94, 1788

55. (a) Beretan, D.N.; Onuchic, J.N., J. Chem. Phys., 1988, 89, 6195; (b) Onuchic, J.N.; Beretan, D.N., J. Phys. Chem., 1988, 92, 4818

56. For example, Fawcett, W.R.; Foss, C., J. Electroanal. Chem., 1989, 270, 103

57. Nielson, R.M.; Weaver, M.J., J. Electroanal. Chem., 1989, 260, 15

58. Nielson, R.M.; Weaver, M.J., Organometallics, 1989, 8, 1636

59. Also consistent with this notion, Wherland et al[60] have observed a k_{ex} value for $Cp_2Ni^{+/o}$ in dichloromethane which is even faster than for $Cp_2Co^{+/o}$; the former couple contains two electrons in the ligand centered HOMO $4e^*_{ig}$ orbital versus one electron for the latter redox system.

60. Gribble, J.D.; Wherland, S., Inorg. Chem., 1990, 29, 1130

61. Weaver, M.J.; McManis, G.E.; Jarzeba, W.; Barbara, P.F., J. Phys. Chem., 1990, 94, 1715

62. Zusman, L.D., Chem. Phys., 1988, 119, 51

63. (a) Fonseca, T., Chem. Phys. Lett., 1989, 162, 491; (b) Fonseca, T., J. Chem. Phys., 1989, 91, 2869

64. The rate constant k_{ex} is obtained from the inverse "average first-passage survival time" τ_a^{-1}, employed in ref. 9.[65]

65. Phelps, D.; Weaver, M.J., in preparation.

66. Ovchinnikova, M. Ya; Russ. Theoret. Exp. Chem., 1981, 17, 507.

67. Phelps, D.; Nelsen, S.; Weaver, M.J., in preparation.

68. For a recent theoretical study, see: Morita, T.; Ladanyi, B.M.; Hynes, J.T., J. Phys. Chem., 1989, 93, 1386

69. (a) McGuire, M.; McLendon, G., J. Phys. Chem., 1986, 90, 2547; (b) Vanthey, E.; Suppan, P., Chem. Phys., 1989, 139, 381; (c) Heitele, H.; Michel-Beyerle, M.E.; Finckh, P., Chem. Phys. Lett., 1987, 138, 237; (d) Harrison, R.J.; Pearce, B.; Beddard, G.S.; Cowan, J.A.; Sanders, J.K.M., Chem. Phys., 1987, 116, 429

70. For example, see: (a) Haim, A., Prog. Inorg. Chem., 1983, 30, 273; (b) Isied, S.S., Prog. Inorg. Chem., 1984, 32, 443

71. (a) Morgan, T.D.; Wolynes, P.G., J. Phys. Chem., 1987, 91, 874; (b) Zusman, L.D., Chem. Phys., 1987, 112, 53

72. (a) Hynes, J.T.; Carter, E.A.; Cicotti, G.; Kim, H.J.; Zichi, D.A.; Ferrario, M.; Kapral, R., in "Perspectives in Photosynthesis", Jortner, J.; Pullman, B., eds, Kluwer Pub., 1990, p.133; (b) Smith, B.B.; Kim, H.J.; Hynes, J.T., in "Condensed Matter Physics Aspects of Electrochemistry," Tosi, M.P.; Kornyshev, A.A., World Scientific Pub., in press (1991).

73. Also of relevance to this issue is the recent theoretical treatment of Kim and Hynes that predicts that the effect of H_{12} in diminishing the barrier height ΔG^* is considerably less than the usually applied formula $\Delta G^* = \Delta G_c^* - H_{12}$, where ΔG_c^* is the cusp barrier height.[72,74] The modification arises from a treatment of the coupling between the electronic polarization and the reactant charge distribution. The corresponding effects on the reaction *dynamics*, however, appear to be small.[74] In addition, a critical limitation of this treatment has recently become apparent.[75]

74. (a) Kim, H.J.; Hynes, J.T., J. Phys. Chem., 1990, 94, 2736; (b) Kim, H.J.; Hynes, J.T., J. Chem. Phys., 1990, 93, 5194,5211

75. Gehlen, J.N.; Chandler, D.; Kim, H.J.; Hynes, J.T., preprint.

76. Zhang, H.; Murray, R.W., J. Am. Chem. Soc., 1991, 113, 5183.

77. For example: Gertner, B.J.; Wilson, K.R.; Hynes, J.T., J. Chem. Phys., 1989, 90, 3537.

78. Kreevoy, M.M.; Kotchevar, A.T., J. Am. Chem. Soc., 1990, 112, 3579

TABLE I Comparison between Inertial Frequencies Estimated from Eq(3) and Inverse Longitudinal Relaxation Times for Some Common Solvents at 25°C

Solvent	τ_L^{-1} [a] ps^{-1}	ω_o [b] ps^{-1}
Acetonitrile	4	11
D_2O	1.9	40
Dimethylsulfoxide	0.5	9.5
Benzonitrile	0.2	4
Hexamethylphosphoramide	0.11	~4
Methanol	(0.135)	11
Ethanol	(0.033)	9.5

[a] Inverse longitudinal relaxation times for solvent indicated, as obtained from dielectric loss data (see ref. 29 for data sources). Values for methanol and ethanol (given in parentheses) refer to large-amplitude, longer time, portion of multicomponent dielectric dispersion.

[b] Estimates of solvent inertial frequency, extracted from Eq(3) (see ref. 30 for data sources).

TABLE II Barrier-Crossing Frequencies, $\kappa_{el}\nu_n(s^{-1})$, for Ferrocenium–Ferrocene Self Exchange in Various Solvents as Estimated from Rate Data by using Theoretical Dielectric Continuum Compared with Experimental Optical Barrier Heights

Solvent	k_{ex}[a] $M^{-1}\ s^{-1}$	ΔG^*_{con}[b] kcal mol^{-1}	ΔG^*_{op}[c] kcal mol^{-1}	τ_L^{-1}[d] s^{-1}	$\kappa_{el}\nu_n(con)$[e] s^{-1}	$\kappa_{el}\nu_n(op)$[f] s^{-1}
Acetonitrile	9×10^6	6.35	5.35	$\sim 3 \times 10^{12}$	1.5×10^{12}	3.0×10^{11}
Propionitrile	9.2×10^6	6.05	5.15	$\sim 3 \times 10^{12}$	1.0×10^{12}	2.2×10^{11}
Acetone	8×10^6	6.0	5.4	3.5×10^{12}	8×10^{11}	4.5×10^{11}
Nitromethane	1.2×10^7	6.0	5.3	4.5×10^{12}	1.2×10^{12}	3.7×10^{11}
Dimethyl-sulfoxide	9.5×10^6	5.4	(4.9)	5×10^{11}	3.5×10^{11}	1.5×10^{11}
Benzonitrile	2.7×10^7	4.8	4.55	2×10^{11}	3.5×10^{11}	2.4×10^{11}
Nitrobenzene	3.0×10^7	4.8	4.55	2×10^{11}	4.0×10^{11}	2.6×10^{11}
Methanol	1.8×10^7	6.45	5.2	(1.3×10^{11})	3.9×10^{12}	4.7×10^{11}
Propylene Carbonate	1.2×10^7	5.85	5.25	(4×10^{11})	8.5×10^{11}	3.4×10^{11}

[a] Rate constant for ferrocenium–ferrocene self exchange (at ionic strength $\mu \simeq 0.01 - 0.02M$), from ref. 29

[b] Barrier height estimated from dielectric continuum formula [Eq(12)], by using a = 3.8Å, $R_h = 2a$. (See refs. 29,43 for other details.) An inner-shell contribution, estimated to be ca 0.6 kcal mol^{-1}, is included.[29]

[c] Barrier height obtained from experimental optical energies ΔE_{op} for bis(ferrocenyl)acetylene cation in given solvent (see ref. 44). Value in parentheses for DMSO is estimated by interpolation.[29]

[d] Inverse longitudinal relaxation time of solvent, taken from compilation in ref. 29. Values in parentheses are for solvents that exhibit additional higher-frequency dispersions.

[e] Estimate of barrier-crossing frequency in given solvent, obtained from k_{ex} value by using Eq(14), assuming that $K_p = 0.25\ M^{-1}$ and setting the barrier height equal to the dielectric-continuum estimate ΔG^*_{con}.

[f] Barrier-crossing frequency, obtained as in footnote e, but by using the optical barrier height ΔG^*_{op} in each solvent.

TABLE III. Comparison between inverse solvent relaxation terms from dielectric loss and TDFS data with effective barrier-crossing frequencies for metallocene self exchanges.

Solvent	ΔG^* [a] kcal mol^{-1}	τ_L^{-1} [b] ps^{-1}	τ_s^{-1} [c] ps^{-1}	$\kappa_{el}\nu_n$, ps^{-1} [d]	
				$Cp^*_2Co^{+/o}$ [e]	$HMFc^{+/o}$ [f]
Acetonitrile	5.35	~3	1.8	2.5	0.2
Acetone	5.4	3.5	1.0 (53%) 3.5 (47%)	2	0.25
Nitromethane	5.3	4.5		3	0.4
Water	5.2	1.9	1.0 (50%) 4.0 (50%)	3.5 [g]	0.35 [g]
Benzonitrile	4.55	0.17	0.16 (61%) 0.47 (39%)	0.3	0.15
Nitrobenzene	4.55	0.19		0.15	0.12
Propylene Carbonate	5.25	(0.3)	0.24 (54%) 2.3 (46%)	1.5	
Methanol	5.2	(0.13)	0.10 (60%) 0.9 (40%)	1.5	0.45

[a] Cusp free-energy barrier for self-exchange reactions, estimated from optical electron-transfer energies for biferrocenylacetylene cation in indicated solvent (see refs. 29 and 44 for details).

[b] Inverse longitudinal relaxation time for solvent indicated, obtained from dielectric loss spectra. See refs. 20 and 29 for data sources.

[c] Inverse solvation times, along with percentage weighting factors, obtained from TDFS data for the coumarin C152 except for water which refers to C343 (refs. 18a,34)

[d] Effective barrier-crossing frequency for metallocene self-exchange reaction indicated, obtained from experimental κ_{el} values together with listed ΔG^* values, assuming that $K_p = 0.25$ M^{-1} [Eq(14)]. See refs. 29 and 61 for kinetic data and other details; ΔG^* values for $Cp^*_2Co^{+/o}$ taken to be 0.5 kcal mol^{-1} smaller to allow for electronic coupling.[29]

[e] $Cp^*_2Co^{+/o}$ = carboxymethyl (cobaltocenium-cobaltocene)[$(CpCO_2Me)_2$ $Co^{+/o}$]

[f] $HMFc^{+/0}$ = hydroxymethyl(ferrocenium-ferrocene)[$Cp.CpCH_2OH)Fe^{+/0}$]

[g] Rate data refers to D_2O.

Figure Captions

Fig. 1

Schematic free energy-reaction coordinate profiles for symmetrical electron-transfer processes having small and large electronic matrix coupling elements, H_{12} (dashed and solid curves, respectively). From ref. 29.

Fig. 2

Plot of dimensionless barrier heights, $\Delta G^*_{os}/2.3RT$ (T = 298K) for metallocene self exchanges versus logarithm of inverse longitudinal relaxation time for eleven "Debye" solvents. Open circles are barrier heights obtained from dielectric-continuum formula [Eq(12)] with a = 3.8Å, R_h = 2a. Filled circles are barrier heights extracted from optical electron-transfer energies, ΔE_{op}, for bis(ferrocenyl) acetylene cation, by $\Delta G^*_{os} = \Delta E_{op}/4$. Latter values given in parentheses are obtained by interpolation (see refs. 42-44 for more details). Key to solvents as given in caption to Fig. 4.

Fig. 3

Logarithmic plots of "barrier-corrected" rate constants ($\underline{M}^{-1}$ s^{-1}, extracted from rate and optical barrier data) versus inverse longitudinal relaxation time (s^{-1}) for five metallocene self-exchange reactions in eleven solvents, taken from ref. 29. See Fig. 4 caption for key to solvents. Key to redox couples: filled circles, $Cp'_2Co^{+/o}$ (Cp' = pentamethylcyclopentadienyl); filled squares, $Cp^*_2Co^{+/o}$ (Cp^* = carboxymethylcyclopentadienyl); filled triangles, $Cp_2Co^{+/o}$; open triangles, $Cp_2Fe^{+/o}$; open squares, hydroxylmethyl(ferrocenium-ferrocene).

Fig. 4

Logarithmic plots of calculated "barrier-corrected" rate constants ($\underline{M}^{-1}$ s^{-1}, for 5.0 kcal mol^{-1} "cusp" barrier), for electron self exchange versus inverse longitudinal relaxation time (s^{-1}) in eleven "Debye" solvents for the sequence of six electronic coupling matrix elements (at reactant contact) as indicated.

See ref. 29 for details. Key to solvents: 1, acetonitrile; 2, propionitrile; 3, acetone; 4, D_2O; 5, nitromethane; 6, dimethylformamide; 7, dimethylsulfoxide; 8, benzonitrile; 9, nitrobenzene; 10, tetramethylurea; 11, hexamethylphosphoramide.

Fig. 5

Illustrative plot of logarithm of rate constant for model electron-exchange reaction, k_{ex} (M^{-1} s^{-1}), versus the inner-shell barrier, ΔG^*_{is} (kcal mol^{-1}), in the presence of varying overdamped solvent dynamics, as calculated[65] from treatment based largely on Marcus et al.[9] Outer-shell barrier held at 4.0 kcal mol^{-1}, solvent inertial frequency $\omega_o = 1 \times 10^{13}$ s^{-1}. Inner-shell frequency, ν_{is}, equal to 5×10^{13} s^{-1} (solid traces), or 5×10^{12} s^{-1} (dashed traces). Upward-going sequence of four traces in each set refer to solvent τ_L^{-1} values of 6×10^{10}, 2×10^{11}, 1×10^{12}, and 6×10^{12} s^{-1} (see refs. 64,65).

FIG 1

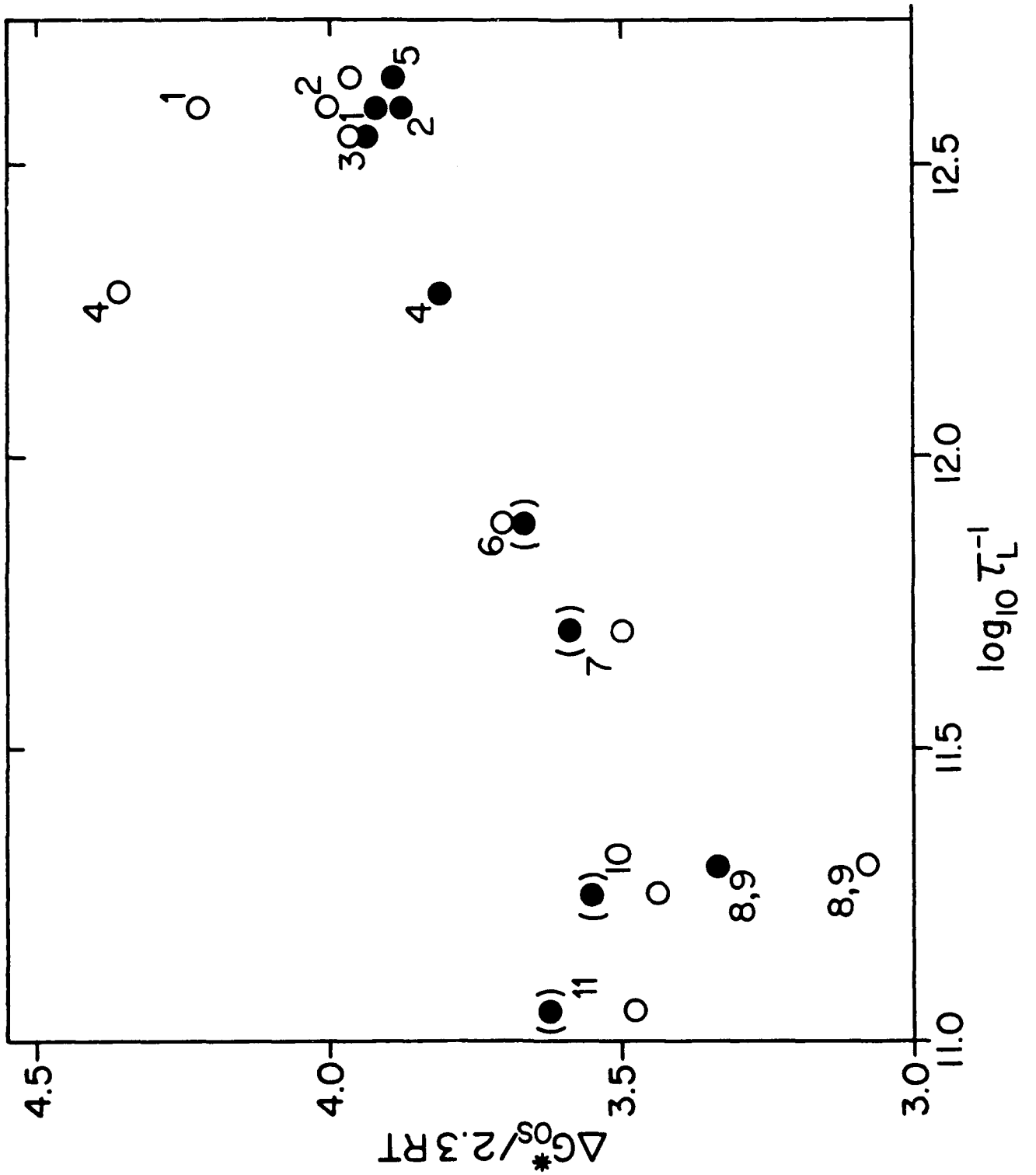
4.5
4.0
3.5
3.0
11.0
11.5
12.0
12.5
$\Delta G^*_{os}/2.3RT$
$\log_{10} \tau_L^{-1}$
1
2
3
4
5
6
7
8,9
8,9
10
11

FIG 2

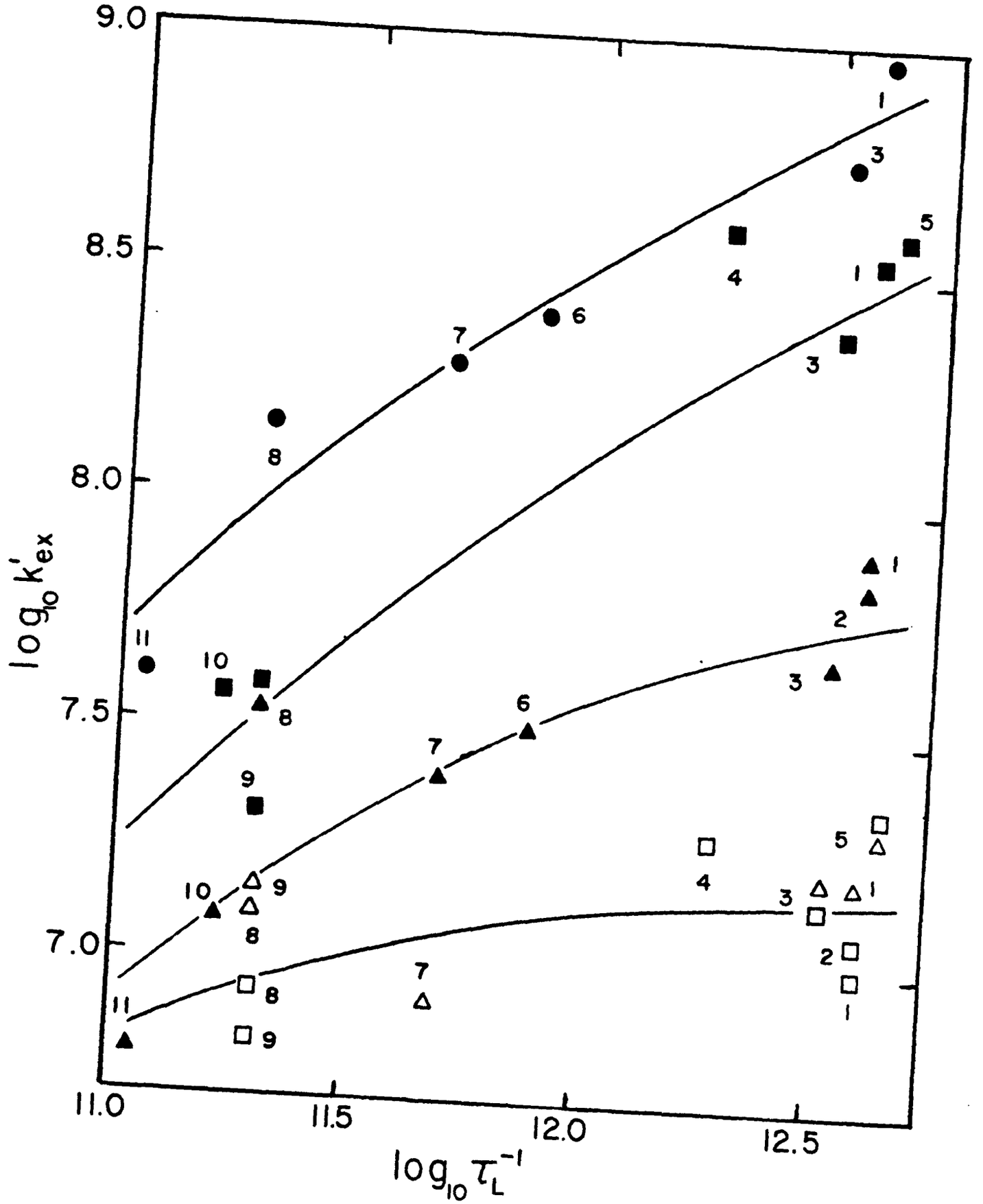

FIG 3

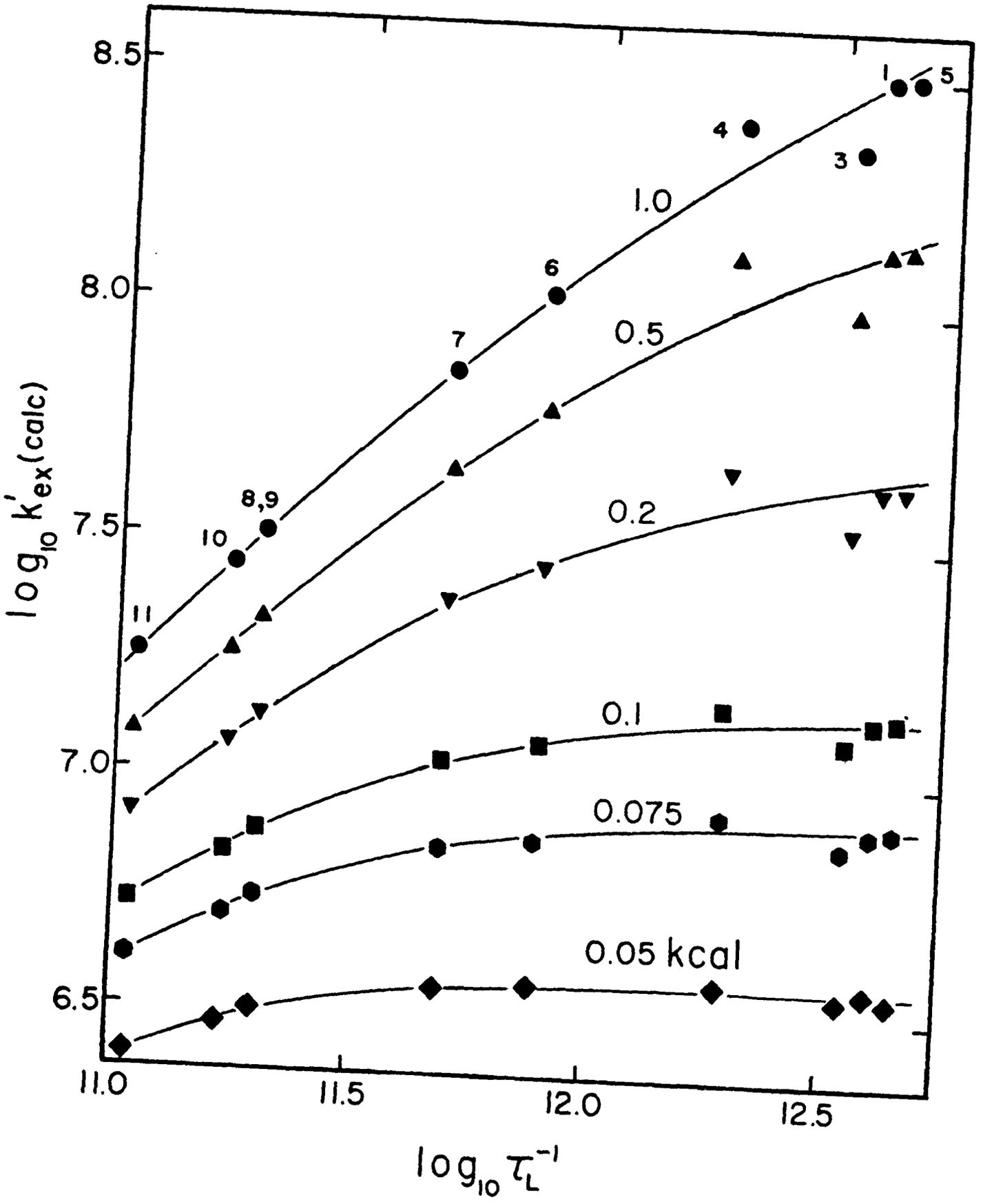
8.5
8.0
7.5
7.0
6.5
11.0
11.5
12.0
12.5
$\log_{10} k'_{ex}(calc)$
$\log_{10} \tau_L^{-1}$
1
5
4
3
1.0
6
7
0.5
8,9
10
11
0.2
0.1
0.075
0.05 kcal

FIG 4

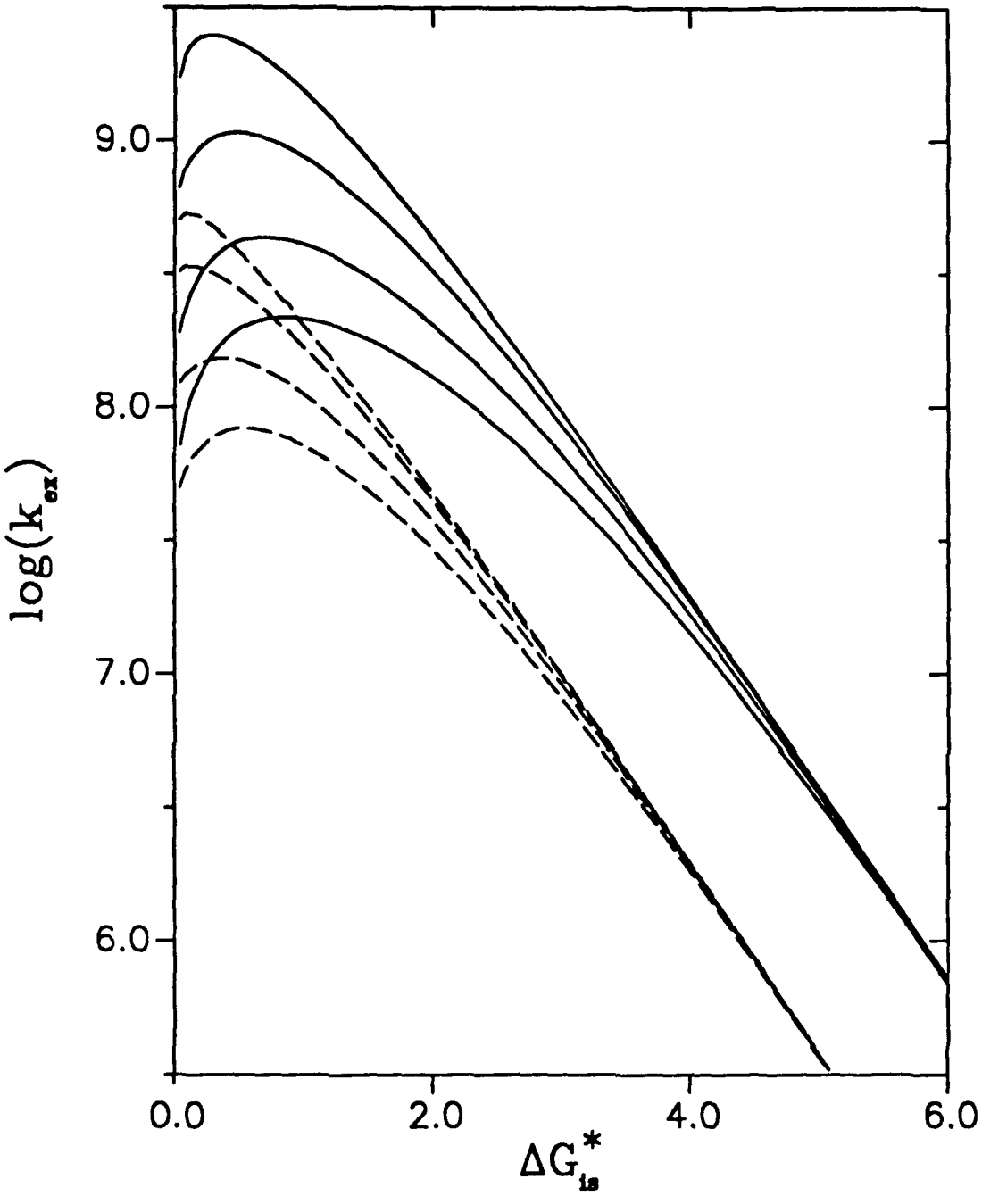

FIG 5